

Active-site loop variations adjust activity and selectivity of the cumene dioxygenase

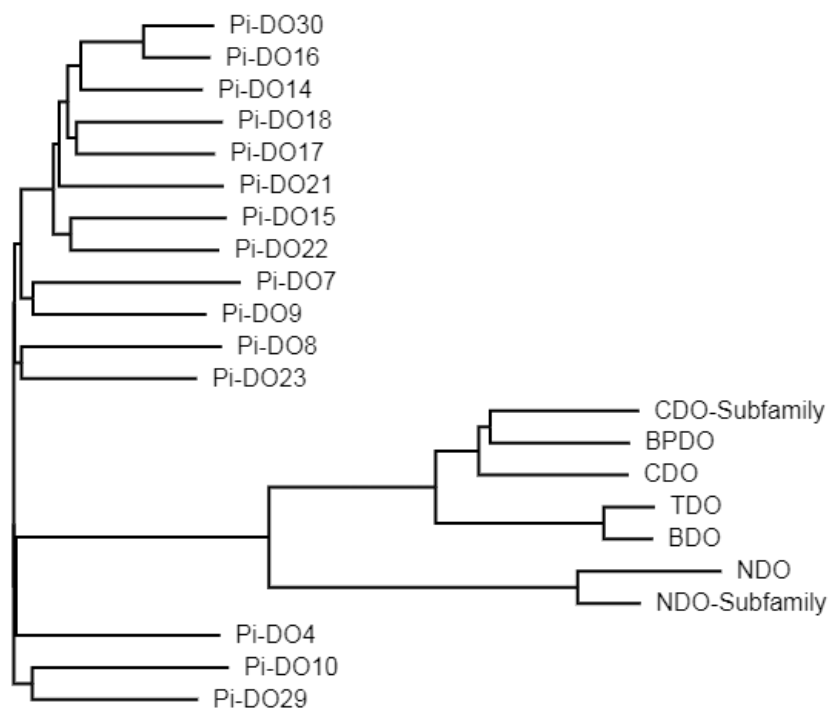
Supplementary Information

Peter M. Heinemann^a, Daniel Armbruster^a and Bernhard Hauer ^{a*}

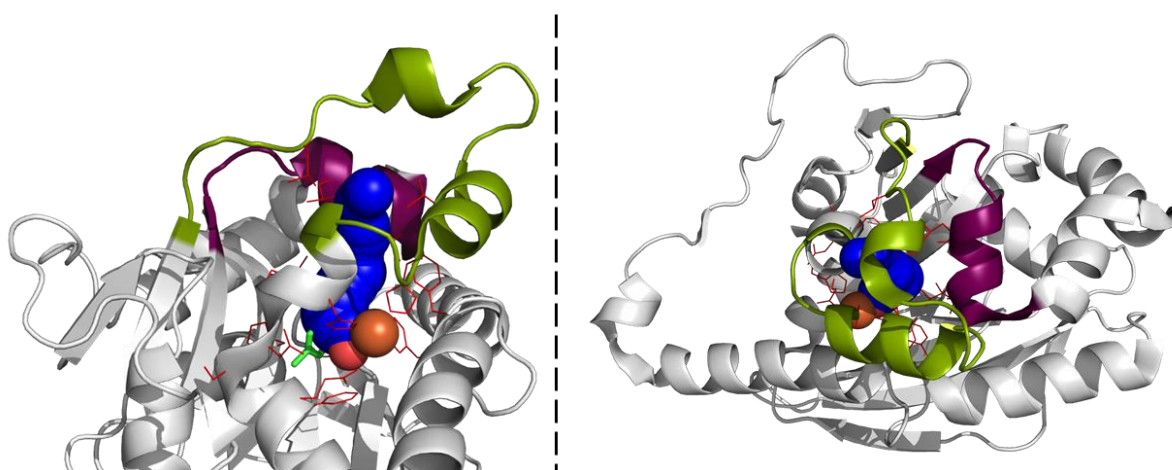
^a Institute of Biochemistry and Technical Biochemistry, Department of Technical Biochemistry, University of Stuttgart, Allmandring 31, 70569 Stuttgart (Germany)

* Corresponding Author

E-mail address: bernhard.hauer@itb.uni-stuttgart.de



Supplementary Fig. 2: Phylogenetic tree of the aligned α -subunits of the oxygenases of CDO, CDO subfamily, BPDO, TDO, BDO, NDO, NDO-subfamily and from *Phenylobacterium immobile* E (Pi-DO).

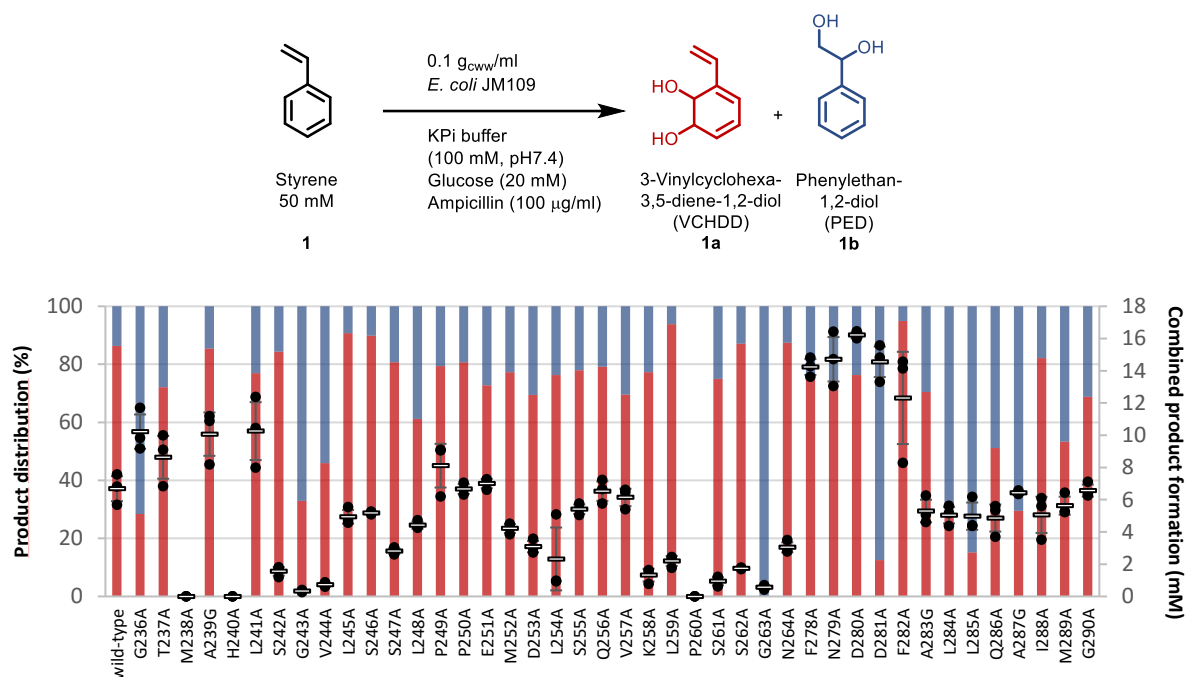


Supplementary Fig. 3: CAVER analysis of the crystal structure of the α -subunit of the CDO oxygenase from *Pseudomonas fluorescens* IP01 (PDB entry 1wql). Side view (left structure) and top view (right structure) of loop 1 (green) and loop 2 (purple) in the crystal structure of one α -subunit (grey) of the CDO oxygenase (PDB entry 1wql). The simulated tunnel (blue), the catalytically active iron (orange sphere), molecular oxygen (red spheres) and active site residues (red sticks) are shown as well as the docked substrate *R*-limonene (green sticks). Iron was selected as starting point with a tunnel radius of 1.2 Å.

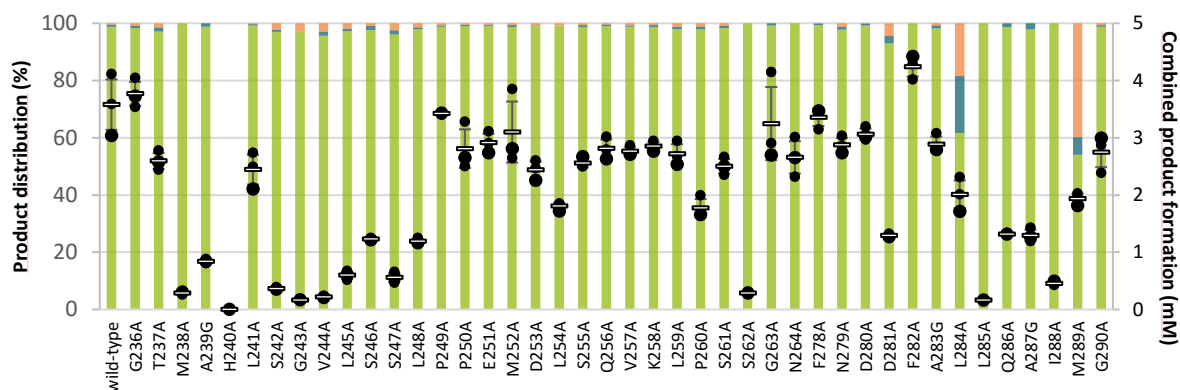
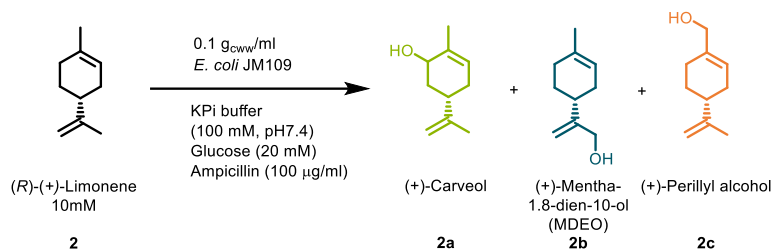
Supplementary Table 1: Conversions of styrene 1, (*R*)-limonene 2 and 2-phenylpyridine 3 with the Wild-type and the variants obtained from the alanine scan of the CDO. Biotransformations were performed in technical triplicates and standard deviations (calculated using Excel version 2016) are indicated. Pf: combined product formation in mM. Regioselectivity in %. Source data are provided as a Source Data file.

	Pf (mM)	Selectivity (%)		Pf (mM)	Selectivity (%)			Pf (mM)	Selectivity (%)	
		1a	1b		2a	2b	2c		3a	3b
Wild-type	6.68 ± 0.77	86.4	13.6	3.56 ± 0.44	98.8	0.7	0.5	0.64 ± 0.03	93.0	7.0
G236A	10.22 ± 1.07	28.4	71.6	3.77 ± 0.21	98.3	0.9	0.8	0.87 ± 0.03	91.7	8.3
T237A	8.63 ± 1.32	72.1	27.9	2.60 ± 0.14	97.1	1.4	1.5	0.90 ± 0.02	94.9	5.1
M238A	0 ± 0	0.0	0.0	0.29 ± 0.02	100.0	0.0	0.0	0 ± 0	0.0	0.0
A239G	10.07 ± 1.35	85.5	14.5	0.84 ± 0.03	98.8	1.2	0.0	0.13 ± 0.01	89.2	10.8
H240A	0 ± 0	0.0	0.0	0 ± 0	0.0	0.0	0.0	0 ± 0	0.0	0.0
L241A	10.26 ± 1.80	77.0	23.0	2.44 ± 0.26	99.3	0.4	0.4	1.41 ± 0.08	92.9	7.1
S242A	1.56 ± 0.26	84.4	15.6	0.37 ± 0.01	97.0	0.8	2.2	0.15 ± 0.01	92.3	7.7
G243A	0.33 ± 0.06	32.9	67.1	0.17 ± 0.00	97.0	0.0	3.0	0.07 ± 0.00	100.0	0.0
V244A	0.73 ± 0.11	45.9	54.1	0.22 ± 0.01	95.7	1.4	2.9	0.09 ± 0.01	89.9	10.1
L245A	4.94 ± 0.43	90.7	9.3	0.60 ± 0.06	97.3	0.9	1.9	0.16 ± 0.01	93.5	6.5
S246A	5.17 ± 0.07	89.9	10.1	1.23 ± 0.02	97.6	1.5	0.9	0.17 ± 0.01	93.7	6.3
S247A	2.81 ± 0.17	80.7	19.3	0.56 ± 0.08	96.1	1.5	2.4	0.15 ± 0.00	93.6	6.4
L248A	4.42 ± 0.21	61.1	38.9	1.19 ± 0.04	97.9	0.6	1.5	0.69 ± 0.06	92.7	7.3
P249A	8.11 ± 1.36	79.4	20.6	3.42 ± 0.02	98.8	0.5	0.7	0.79 ± 0.00	93.4	6.6
P250A	6.66 ± 0.30	80.8	19.2	2.81 ± 0.34	99.0	0.4	0.5	0.89 ± 0.02	93.1	6.9
E251A	7.00 ± 0.29	72.7	27.3	2.92 ± 0.15	99.2	0.3	0.6	0.68 ± 0.02	93.1	6.9
M252A	4.22 ± 0.28	77.3	22.7	3.10 ± 0.53	98.7	0.7	0.7	0.66 ± 0.02	93.2	6.8
D253A	3.09 ± 0.35	69.5	30.5	2.44 ± 0.14	99.1	0.2	0.7	0.41 ± 0.03	95.4	4.6
L254A	2.32 ± 1.95	76.3	23.7	1.81 ± 0.06	99.2	0.0	0.8	0.57 ± 0.04	95.1	4.9

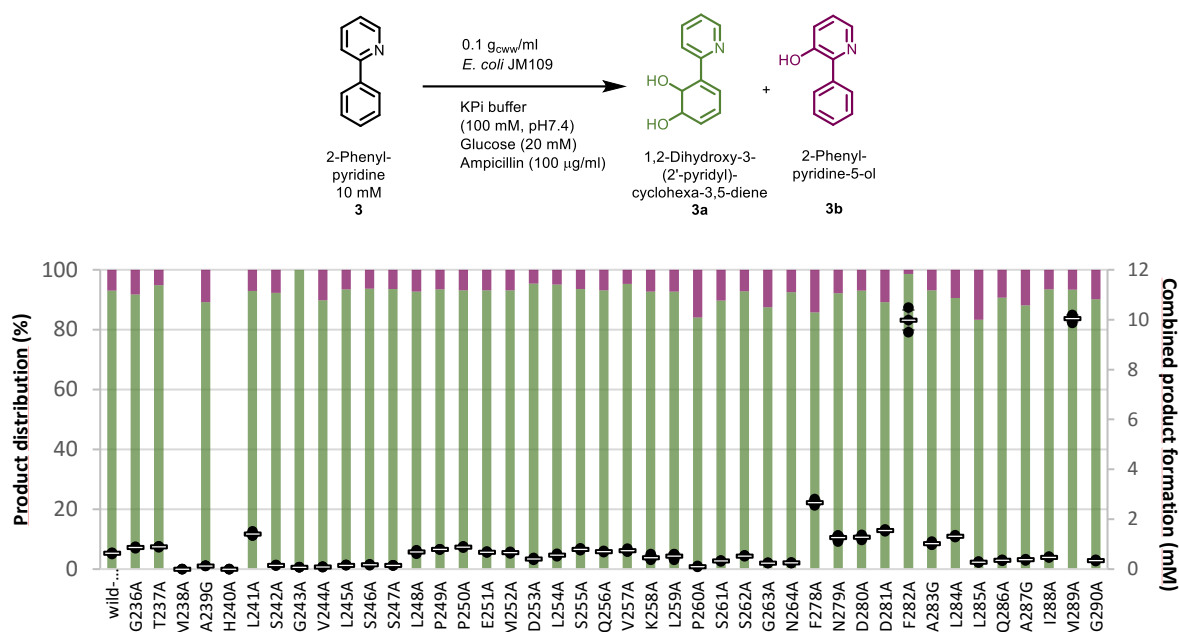
S255A	5.41 ± 0.29	77.9	22.1	2.56 ± 0.08	98.7	0.6	0.6	0.80 ± 0.03	93.5	6.5
Q256A	6.53 ± 0.60	79.1	20.9	2.81 ± 0.16	99.0	0.6	0.4	0.71 ± 0.02	93.2	6.8
V257A	6.14 ± 0.54	69.6	30.4	2.77 ± 0.07	98.8	0.4	0.8	0.74 ± 0.05	95.3	4.7
K258A	1.32 ± 0.40	77.3	22.7	2.85 ± 0.07	98.7	0.6	0.7	0.46 ± 0.10	92.7	7.3
L259A	2.20 ± 0.31	93.8	6.2	2.72 ± 0.17	97.9	0.8	1.2	0.53 ± 0.11	92.8	7.2
P260A	0 ± 0	0.0	0.0	1.78 ± 0.15	97.9	1.0	1.1	0.11 ± 0.01	84.0	16.0
S261A	0.94 ± 0.25	74.9	25.1	2.50 ± 0.13	98.3	0.8	0.9	0.33 ± 0.02	89.7	10.3
S262A	1.73 ± 0.04	87.2	12.8	0.29 ± 0.01	100.0	0.0	0.0	0.53 ± 0.01	92.9	7.1
G263A	0.56 ± 0.11	0.0	100.0	3.25 ± 0.64	99.3	0.7	0.0	0.25 ± 0.00	87.5	12.5
N264A	3.04 ± 0.31	87.4	12.6	2.66 ± 0.28	100.0	0.0	0.0	0.25 ± 0.01	92.5	7.5
F278A	14.24 ± 0.49	75.8	24.2	3.36 ± 0.15	99.3	0.5	0.1	2.67 ± 0.11	85.8	14.2
N279A	14.71 ± 1.38	73.7	26.3	2.88 ± 0.12	97.8	1.0	1.2	1.26 ± 0.11	92.2	7.8
D280A	16.21 ± 0.18	76.3	23.7	3.06 ± 0.10	99.2	0.7	0.1	1.28 ± 0.09	93.1	6.9
D281A	14.56 ± 0.94	12.6	87.4	1.29 ± 0.02	93.0	2.6	4.4	1.56 ± 0.03	89.2	10.8
F282A	12.31 ± 2.86	95.0	5.0	4.24 ± 0.17	100.0	0.0	0.0	9.99 ± 0.40	98.6	1.4
A283G	5.30 ± 0.70	70.5	29.5	2.89 ± 0.13	98.2	0.9	0.8	1.02 ± 0.06	93.1	6.9
L284A	5.04 ± 0.51	27.9	72.1	2.01 ± 0.24	61.6	20.1	18.3	1.32 ± 0.04	90.5	9.5
L285A	4.98 ± 0.85	15.2	84.8	0.16 ± 0.00	100.0	0.0	0.0	0.28 ± 0.02	83.3	16.7
Q286A	4.87 ± 0.84	51.1	48.9	1.32 ± 0.01	98.7	1.3	0.0	0.36 ± 0.02	90.7	9.3
A287G	6.42 ± 0.11	29.5	70.5	1.29 ± 0.10	97.8	2.2	0.0	0.38 ± 0.02	88.2	11.8
I288A	5.06 ± 1.12	82.2	17.8	0.45 ± 0.03	100.0	0.0	0.0	0.48 ± 0.01	93.5	6.5
M289A	5.63 ± 0.56	53.3	46.7	1.94 ± 0.09	54.1	6.2	39.8	10.05 ± 0.13	93.3	6.7
G290A	6.57 ± 0.37	68.8	31.2	2.75 ± 0.26	98.8	0.6	0.6	0.35 ± 0.02	90.1	9.9



Supplementary Fig. 4: Product distribution and formation of the two products 3-vinylcyclohexa-3,5-diene-1,2-diol 1a (VCHDD, red, bottom bars) and phenylethan-1,2-diol 1b (PED, blue, top bars) for the biotransformation of styrene with the wild-type and variants obtained from the alanine scan of loop 1 and 2 of the CDO. The reactions were performed in technical triplicates (black dots) with average values (horizontal bar) and standard deviations (calculated using Excel version 2016) indicated. Source data are provided as a Source Data file.



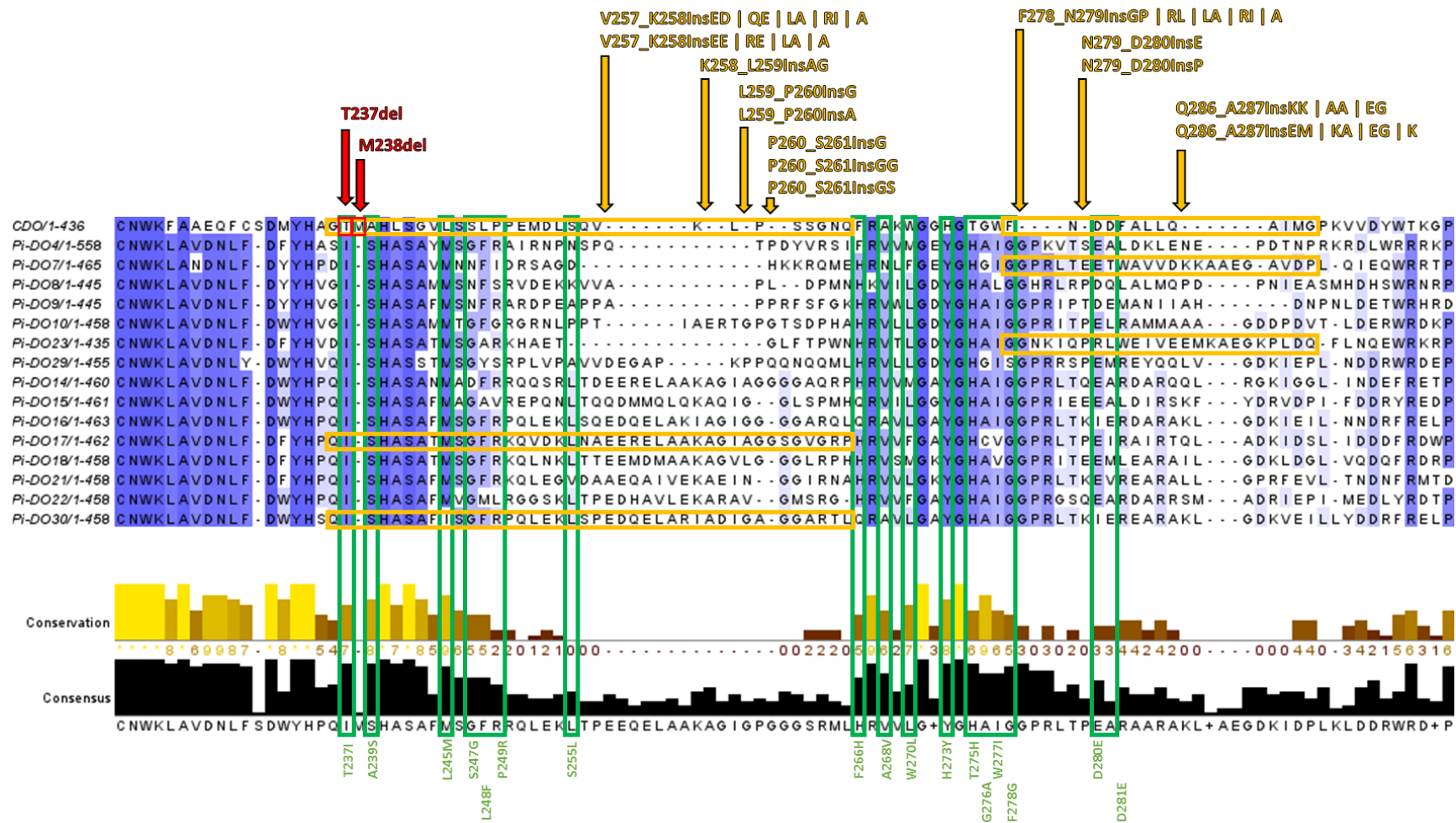
Supplementary Fig. 5: Product distribution and formation of the products (+)-carveol 2a (green, bottom bars), (+)-mentha-1,8-dien-10-ol 2b (MDEO, blue, middle bars) and (+)-perillyl alcohol 2c (orange, top bars) for the biotransformation of (*R*)-limonene 2 with the wild-type and variants obtained from the alanine scan of loop 1 and 2 of the CDO. The reactions were performed in technical triplicates (black dots) with average values (horizontal bar) and standard deviations (calculated using Excel version 2016) indicated. Source data are provided as a Source Data file.



Supplementary Fig. 6: Product distribution of the products 1,2-dihydroxy-3-(2'-pyridyl)cyclohexa-3,5-diene 3a (green, bottom bars) and 2-phenylpyridine-5-ol 3b (purple, top bars) for the biotransformation of 2-phenylpyridine 3 with the wild-type and variants obtained from the alanine scan of loop 1 and 2 of the CDO. The reactions were performed in technical triplicates (black dots) with average values (horizontal bar) and standard deviations (calculated using Excel version 2016) indicated. Source data are provided as a Source Data file.

Supplementary Table 2: Conversion of styrene 1, (*R*)-limonene 2 and 2-phenylpyridine 3 with the Wild-type and selected saturation variants. Biotransformations were performed in technical triplicates and standard deviation (calculated using Excel version 2016) are indicated. Pf: combined product formation in mM. Regioselectivity in %. Source data are provided as a Source Data file.

	Pf (mM)	Selectivity (%)		Pf (mM)	Selectivity (%)			Pf (mM)	Selectivity (%)	
		1a	1b		2a	2b	2c		3a	3b
Wild-type	6.68 ± 0.77	86.4	13.6	3.58 ± 0.44	98.8	0.7	0.5	0.64 ± 0.03	93.0	7.0
F278V	0.24 ± 0.07	100.0	0.0	5.31 ± 0.79	100.0	0.0	0.0	1.57 ± 0.04	94.1	5.9
F282V	1.31 ± 0.06	69.4	30.6	5.15 ± 0.28	100.0	0.0	0.0	1.28 ± 0.02	97.0	3.0
F282T	0.05 ± 0.00	100.0	0.0	2.78 ± 0.24	100.0	0.0	0.0	9.82 ± 0.20	97.3	2.7
L284G	0.31 ± 0.08	84.7	15.3	2.08 ± 0.19	30.8	19.4	49.7	0.74 ± 0.04	91.4	8.6
Q286F	0.65 ± 0.05	67.5	32.5	1.86 ± 0.16	100.0	0.0	0.0	0.40 ± 0.05	93.8	6.2
I288S	0.02 ± 0.03	41.6	58.4	1.31 ± 0.41	69.9	3.5	26.5	1.11 ± 0.03	93.3	6.7
I288T	0.10 ± 0.01	73.9	26.1	2.14 ± 0.20	96.4	0.1	3.4	1.96 ± 0.02	93.6	6.4
M289K	0.09 ± 0.01	0.0	100.0	0.06 ± 0.00	100.0	0.0	0.0	0.15 ± 0.01	86.7	13.3



Supplementary Fig. 7: Excerpt of the sequence alignment of CDO with α -subunits of the oxygenases from *Phenylobacterium immobile* E and variant selection for the adaption library. Single point mutations are indicated in green, single point deletions in red. Introduced sequence-alignment based insertions are highlighted in yellow, the loops 1 and 2 of the CDO together with the longest corresponding loops from oxygenases originated from *Phenylobacterium immobile* E are framed in yellow. Slashes in the variant designation represent stepwise insertions

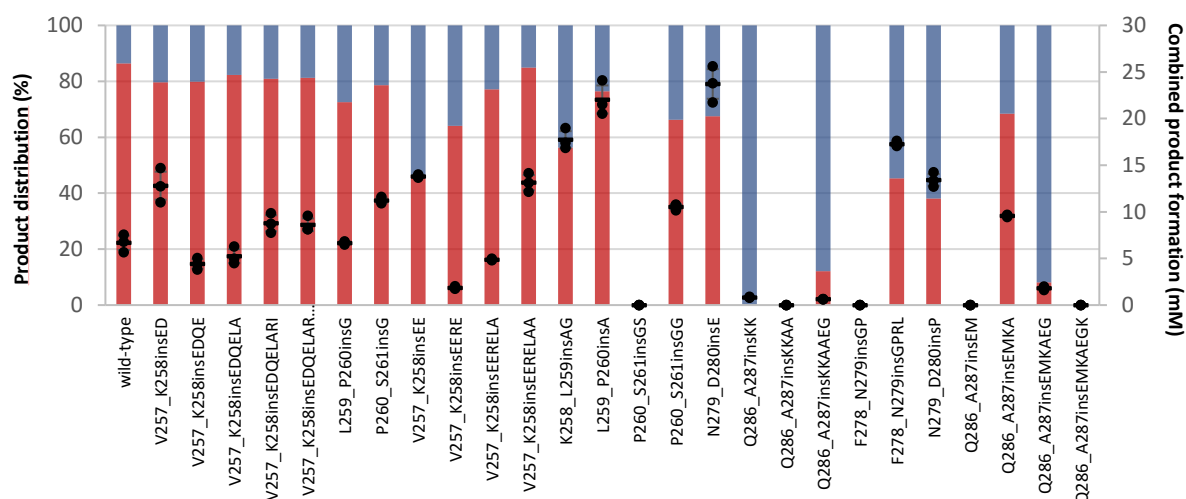
Supplementary Table 3: Conversions of styrene 1, (*R*)-limonene 2 and 2-phenylpyridine 3 with the wild-type, and deletion and single-point mutation variants based on loops in oxygenases from *Phenylbacterium immobile* E. Biotransformations were performed in technical triplicates and standard deviation (calculated using Excel version 2016) are indicated. Pf: combined product formation in mM. Regioselectivity in %. Source data are provided as a Source Data file.

	Pf (mM)	Selectivity (%)		Pf (mM)	Selectivity (%)			Pf (mM)	Selectivity (%)	
		1a	1b		2a	2b	2c		3a	3b
Wild-type	6.68 ± 0.77	86.4	13.6	3.58 ± 0.44	98.8	0.7	0.5	0.64 ± 0.03	93.0	7.0
T237del	0 ± 0	0.0	0.0	0 ± 0	0.0	0.0	0.0	0 ± 0	0.0	0.0
M238del	0 ± 0	0.0	0.0	0.12 ± 0.00	100.0	0.0	0.0	0 ± 0	0.0	0.0
T237I	7.99 ± 0.13	78.5	21.5	0.44 ± 0.03	100.0	0.0	0.0	0.06 ± 0.01	100.0	0.0
A239S	6.89 ± 0.21	69.8	30.2	0.86 ± 0.02	97.4	0.8	1.8	0.55 ± 0.02	91.0	9.0
L245M	0 ± 0	0.0	0.0	0.10 ± 0.00	100.0	0.0	0.0	0 ± 0	0.0	0.0
S247G	0 ± 0	0.0	0.0	0 ± 0	0.0	0.0	0.0	0 ± 0	0.0	0.0
L248F	0 ± 0	0.0	0.0	0 ± 0	0.0	0.0	0.0	0 ± 0	0.0	0.0
P249R	0 ± 0	0.0	0.0	0 ± 0	0.0	0.0	0.0	0 ± 0	0.0	0.0
S255L	5.35 ± 0.10	71.8	28.2	0.58 ± 0.02	96.7	2.3	1.0	0.05 ± 0.01	81.4	18.6
F266H	8.14 ± 0.42	75.8	24.2	1.38 ± 0.02	98.0	0.9	1.1	0.11 ± 0.01	86.6	13.4
A268V	4.18 ± 0.07	73.6	26.4	0.84 ± 0.06	97.4	1.9	0.7	0 ± 0	0.0	0.0
W270L	2.52 ± 0.12	84.4	15.6	2.74 ± 0.41	99.1	0.4	0.5	0.22 ± 0.02	92.4	7.6
H273Y	0 ± 0	0.0	0.0	0.14 ± 0.00	100.0	0.0	0.0	0 ± 0	0.0	0.0
T275H	1.46 ± 0.07	84.4	15.6	1.39 ± 0.02	99.2	0.4	0.5	0.51 ± 0.01	95.4	4.6
G276A	0 ± 0	0.0	0.0	1.22 ± 0.06	100.0	0.0	0.0	0.19 ± 0.01	92.1	7.9
W277I	0 ± 0	0.0	0.0	0 ± 0	0.0	0.0	0.0	0 ± 0	0.0	0.0
F278G	0.93 ± 0.13	75.5	24.5	2.12 ± 0.05	96.7	0.9	2.4	0.49 ± 0.02	86.2	13.8
D280E	2.24 ± 0.04	89.1	10.9	3.21 ± 0.18	99.5	0.5	0.0	0.37 ± 0.01	93.4	6.6
D281E	14.25 ± 0.49	55.9	44.1	0.64 ± 0.03	100.0	0.0	0.0	0.07 ± 0.01	90.9	9.1

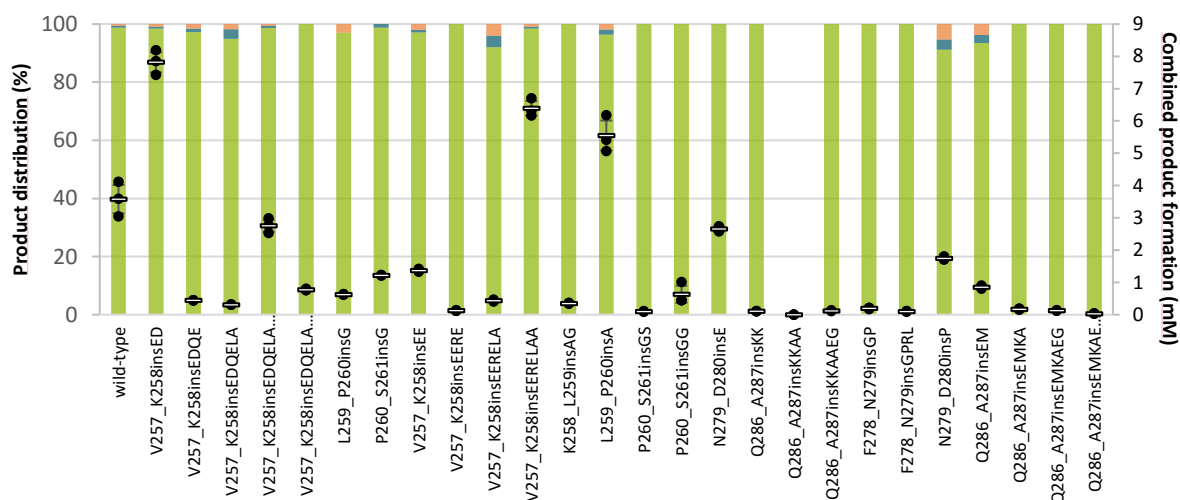
Supplementary Table 4: Conversions of styrene 1, (R)-limonene 2 and 2-phenylpyridine 3 with the wild-type and insertion variants based on loops in oxygenases from *Phenylobacterium immobile* E. Biotransformations were performed in technical triplicates and standard deviations (calculated using Excel version 2016) are indicated. Pf: combined product formation in mM. Regioselectivity in %. Source data are provided as a Source Data file.

	Pf (mM)	Selectivity (%)		Pf (mM)	Selectivity (%)			Pf (mM)	Selectivity (%)	
		1a	1b		2a	2b	2c		3a	3b
Wild-type	6.68 ± 0.77	86.4	13.6	3.58 ± 0.44	98.8	0.7	0.5	0.64 ± 0.03	93.0	7.0
V257_K258 insED	12.81 ± 1.50	79.7	20.3	7.81 ± 0.31	98.4	0.7	0.9	0.64 ± 0.05	92.8	7.2
V257_K258 insEDQE	4.42 ± 0.50	79.9	20.1	0.44 ± 0.01	97.3	1.2	1.5	0.08 ± 0.01	89.8	10.2
V257_K258 insEDQELA	5.25 ± 0.74	82.3	17.7	0.314 ± 0.00	95.0	3.2	1.8	0.09 ± 0.01	90.1	9.9
V257_K258 insEDQELA RI	8.78293 ± 0.86	81.0	19.0	2.75 ± 0.19	98.6	0.8	0.6	0.42 ± 0.02	94.9	5.1
V257_K258 insEDQELA RIA	8.61 ± 0.68	81.3	18.7	0.77 ± 0.02	100.0	0.0	0.0	0.38 ± 0.12	94.7	5.3
L259_P260 insG	6.68 ± 0.15	72.6	27.4	0.62 ± 0.01	97.0	0.0	3.0	0.12 ± 0.00	91.2	8.8
P260_S261 insG	11.23 ± 0.29	78.6	21.4	1.22 ± 0.01	98.7	1.3	0.0	0.10 ± 0.01	92.5	7.5
V257_K258 insEE	13.81 ± 0.15	46.5	53.5	1.37 ± 0.04	97.2	0.9	2.0	0.10 ± 0.01	91.7	8.3
V257_K258 insEERE	1.86 ± 0.11	64.0	36.0	0.12 ± 0.01	100.0	0.0	0.0	0 ± 0	0.0	0.0
V257_K258 insEERELA	4.88 ± 0.07	77.2	22.8	0.43 ± 0.03	92.1	3.9	4.0	0.12 ± 0.01	90.2	9.8
V257_K258 insEERELA A	13.14 ± 0.82	84.9	15.1	6.39 ± 0.23	98.4	0.7	1.0	1.97 ± 0.13	96.2	3.8
K258_L259 insAG	17.75 ± 0.91	56.3	43.7	0.35 ± 0.01	100.0	0.0	0.0	0.26 ± 0.01	91.7	8.3
L259_P260 insA	22.06 ± 1.51	76.4	23.6	5.55 ± 0.46	96.3	1.7	1.9	1.05 ± 0.07	92.5	7.5
P260_S261 insGS	0 ± 0	0.0	0.0	0.092 ± 0.01	100.0	0.0	0.0	0 ± 0	0.0	0.0
P260_S261 insGG	10.55 ± 0.27	66.2	33.8	0.63 ± 0.27	100.0	0.0	0.0	0.07 ± 0.01	92.3	7.7
N279_D280 insE	23.72 ± 1.59	67.5	32.5	2.65 ± 0.07	100.0	0.0	0.0	1.03 ± 0.10	91.9	8.1
Q286_A287 insKK	0.83 ± 0.05	0.0	100.0	0.10 ± 0.00	100.0	0.0	0.0	0 ± 0	0.0	0.0
Q286_A287 insKKAA	0 ± 0	0.0	0.0	0 ± 0	0.0	0.0	0.0	0 ± 0	0.0	0.0
Q286_A287 insKKAAEG	0.64 ± 0.02	12.2	87.8	0.12 ± 0.01	100.0	0.0	0.0	0 ± 0	0.0	0.0

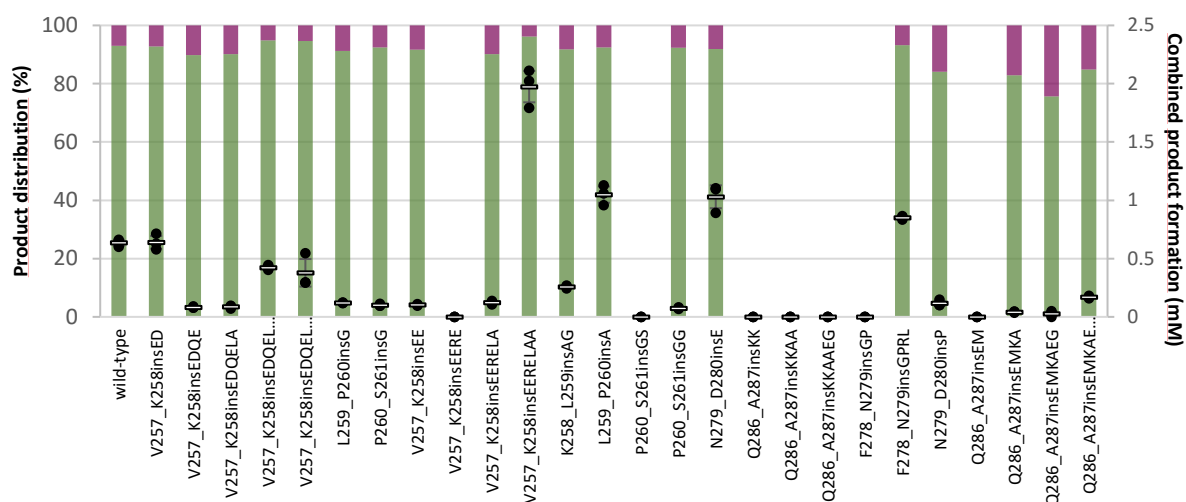
F278_N279 insGP	0 ± 0	0.0	0.0	0.19 ± 0.02	100.0	0.0	0.0	0 ± 0	0.0	0.0
F278_N279 insGPRL	17.28 ± 0.23	45.3	54.7	0.10 ± 0.01	100.0	0.0	0.0	0.85 ± 0.01	93.2	6.8
N279_D280 insP	13.437 ± 0.63	38.1	61.9	1.74 ± 0.04	91.2	3.6	5.3	0.12 ± 0.02	84.1	15.9
Q286_A287 insEM	0 ± 0	0.0	0.0	0.85 ± 0.04	93.5	2.7	3.8	0 ± 0	0.0	0.0
Q286_A287 insEMKA	9.59 ± 0.10	68.4	31.6	0.16 ± 0.02	100.0	0.0	0.0	0.04 ± 0.00	82.8	17.2
Q286_A287 insEMKAE G	1.81 ± 0.14	8.2	91.8	0.13 ± 0.01	100.0	0.0	0.0	0.03 ± 0.02	75.7	24.3
Q286_A287 insEMKAE GK	0 ± 0	0.0	0.0	0.03 ± 0.00	100.0	0.0	0.0	0.17 ± 0.01	84.8	15.2



Supplementary Fig. 8: Product distribution and formation of the two products 3-vinylcyclohexa-3,5-diene-1,2-diol 1a (VCHDD, red, bottom bars) and phenylethan-1,2-diol 1b (PED, blue, top bars) for the biotransformation of styrene with the wild-type and insertion variants based on loops in oxygenases from *Phenyllobacterium immobile* E. The reactions were performed in technical triplicates (black dots) with average values (horizontal bar) and standard deviations (calculated using Excel version 2016) indicated. Source data are provided as a Source Data file.



Supplementary Fig. 9: Product distribution and formation of the products (+)-carveol 2a (green, bottom bars), (+)-mentha-1,8-dien-10-ol 2b (MDEO, blue, middle bars) and (+)-perillyl alcohol 2c (orange, top bars) for the biotransformation of (*R*)-limonene 2 with the wild-type and insertion variants based on loops in oxygenases from *Phenyllobacterium immobile* E. The reactions were performed in technical triplicates (black dots) with average values (horizontal bar) and standard deviations (calculated using Excel version 2016) indicated. Source data are provided as a Source Data file.



Supplementary Fig. 10: Product distribution and formation of the products 1,2-dihydroxy-3-(2'-pyridyl)cyclohexa-3,5-diene 3a (green, bottom bars) and 2-phenylpyridine-5-ol 3b (purple, top bars) for the biotransformation of 2-phenylpyridine 3 with the wild-type and insertion variants based on loops in oxygenases from in *Phenylbacterium immobile* E. The reactions were performed in technical triplicates (black dots) with average values (horizontal bar) and standard deviations (calculated using Excel version 2016) indicated. Source data are provided as a Source Data file.

Supplementary Table 5: Conversions of styrene 1, (*R*)-limonene 2 and 2-phenylpyridine 3 with the wild-type and deletion variants. Biotransformations were performed in technical triplicates and standard deviations (calculated using Excel version 2016) are indicated. Pf: combined product formation in mM. Regioselectivity in %. Source data are provided as a Source Data file.

	Pf (mM)	Selectivity (%)		Pf (mM)	Selectivity (%)			Pf (mM)	Selectivity (%)	
		1a	1b		2a	2b	2c		3a	3b
Wild-type	6.68 ± 0.77	86.4	13.6	3.58 ± 0.44	98.8	0.7	0.5	0.64 ± 0.03	93.0	7.0
E251del	13.14 ± 2.74	84.5	15.5	3.38 ± 0.21	97.2	1.3	1.5	2.18 ± 0.21	94.7	5.3
P250_M252 del	12.57 ± 2.20	82.4	17.6	2.01 ± 0.16	96.3	1.6	2.1	2.74 ± 0.10	94.2	5.8
L248_L254 del	0 ± 0	0.0	0.0	0.17 ± 0.00	100.0	0.0	0.0	0 ± 0	0.0	0.0
V257del	13.36 ± 0.54	77.1	22.9	2.57 ± 0.16	96.6	1.2	2.1	2.49 ± 0.049	93.6	6.4
Q256_K258 del	15.26 ± 0.56	44.1	55.9	3.68 ± 0.16	97.4	1.1	1.6	1.96 ± 0.04	91.5	8.5
L254_P260 del	0 ± 0	0.0	0.0	0.04 ± 0.00	100.0	0.0	0.0	0 ± 0	0.0	0.0
A283del	15.82 ± 1.99	89.2	10.8	8.92 ± 0.80	98.2	0.8	1.0	10.16 ± 0.47	98.7	1.3
F282_L284 del	19.93 ± 1.97	6.3	93.7	0.60 ± 0.02	100.0	0.0	0.0	3.68 ± 0.11	93.0	7.0
D280_Q286 del	0 ± 0	0.0	0.0	0 ± 0	0.0	0.0	0.0	0 ± 0	0.0	0.0

Supplementary Table 6: Conversions of styrene 1, (*R*)-limonene 2 and 2-phenylpyridine 3 with the wild-type and insertion variants after V257 based on LILI. Biotransformations were performed in technical triplicates and standard deviations (calculated using Excel version 2016) are indicated. Pf: combined product formation in mM. Regioselectivity in %. Source data are provided as a Source Data file.

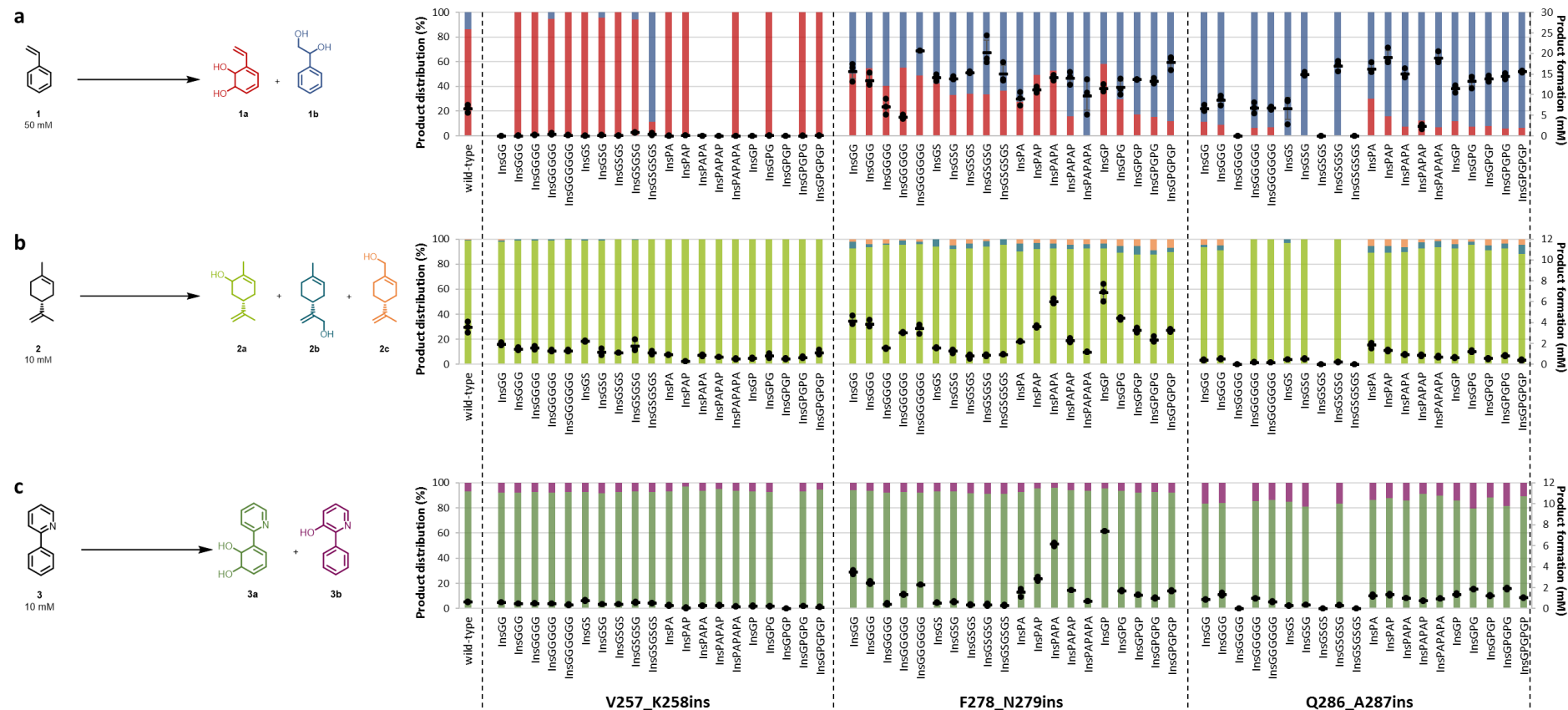
	Pf (mM)	Selectivity (%)		Pf (mM)	Selectivity (%)			Pf (mM)	Selectivity (%)	
		1a	1b		2a	2b	2c		3a	3b
Wild-type	6.68 ± 0.77	86.4	13.6	3.58 ± 0.44	98.8	0.7	0.5	0.64 ± 0.03	93.0	7.0
V257_K258 insGG	0 ± 0	0.0	0.0	1.96 ± 0.11	97.6	1.2	1.2	0.61 ± 0.00	92.2	7.8
V257_K258 insGGG	0.07 ± 0.01	100.0	0.0	1.49 ± 0.11	98.8	1.2	0.0	0.48 ± 0.01	92.1	7.9
V257_K258 insGGGG	0.22 ± 0.07	100.0	0.0	1.61 ± 0.14	98.9	1.1	0.0	0.52 ± 0.02	92.5	7.5
V257_K258 insGGGGG	0.49 ± 0.22	94.8	5.2	1.32 ± 0.08	98.6	1.4	0.0	0.51 ± 0.01	92.1	7.9
V257_K258 insGGGGG G	0.17 ± 0.09	100.0	0.0	1.32 ± 0.08	99.8	0.2	0.0	0.37 ± 0.03	92.8	7.2
V257_K258 insGS	0.05 ± 0.02	100.0	0.0	2.22 ± 0.04	98.8	1.2	0.0	0.77 ± 0.05	92.6	7.4
V257_K258 insGSG	0.22 ± 0.10	95.6	4.4	1.19 ± 0.27	98.8	1.2	0.0	0.41 ± 0.01	91.6	8.4
V257_K258 insGSGS	0.09 ± 0.03	100.0	0.0	1.13 ± 0.01	100.0	0.0	0.0	0.43 ± 0.02	92.7	7.3
V257_K258 insGSGSG	0.87 ± 0.11	94.1	5.9	1.75 ± 0.47	99.4	0.6	0.0	0.58 ± 0.05	93.1	6.9
V257_K258 insGSGSGS	0.41 ± 0.29	11.3	88.7	1.126 ± 0.16	100.0	0.0	0.0	0.52 ± 0.03	92.5	7.5
V257_K258 insPA	0.03 ± 0.04	100.0	0.0	0.95 ± 0.04	100.0	0.0	0.0	0.31 ± 0.03	92.9	7.1
V257_K258 insPAP	0.10 ± 0.02	100.0	0.0	0.33 ± 0.02	100.0	0.0	0.0	0.08 ± 0.05	97.0	3.0
V257_K258 insPAPA	0 ± 0	0.0	0.0	0.88 ± 0.07	100.0	0.0	0.0	0.27 ± 0.02	93.7	6.3
V257_K258 insPAPAP	0 ± 0	0.0	0.0	0.73 ± 0.01	100.0	0.0	0.0	0.31 ± 0.04	94.9	5.1
V257_K258 insPAPAPA	0.01 ± 0.02	100.0	0.0	0.55 ± 0.06	100.0	0.0	0.0	0.22 ± 0.02	93.5	6.5
V257_K258 insGP	0 ± 0	0.0	0.0	0.58 ± 0.04	100.0	0.0	0.0	0.25 ± 0.05	93.2	6.8
V257_K258 insGPG	0.10 ± 0.04	100.0	0.0	0.84 ± 0.18	100.0	0.0	0.0	0.24 ± 0.01	92.5	7.5
V257_K258 insGPGP	0 ± 0	0.0	0.0	0.58 ± 0.04	100.0	0.0	0.0	0 ± 0	0.0	0.0
V257_K258 insGPGPG	0.07 ± 0.02	100.0	0.0	0.67 ± 0.07	100.0	0.0	0.0	0.27 ± 0.01	93.1	6.9
V257_K258 insGPGPGP	0.09 ± 0.02	100.0	0.0	1.15 ± 0.20	100.0	0.0	0.0	0.17 ± 0.02	94.4	5.6

Supplementary Table 7: Conversions of styrene 1, (*R*)-limonene 2 and 2-phenylpyridine 3 with the wild-type and insertion variants after F278 based on LILI. Biotransformations were performed in technical triplicates and standard deviations (calculated using Excel version 2016) are indicated. Pf: combined product formation in mM. Regioselectivity in %. Source data are provided as a Source Data file.

	Pf (mM)	Selectivity (%)		Pf (mM)	Selectivity (%)			Pf (mM)	Selectivity (%)	
		1a	1b		2a	2b	2c		3a	3b
Wild-type	6.68 ± 0.77	86.4	13.6	3.58 ± 0.44	98.8	0.7	0.5	0.64 ± 0.03	93.0	7.0
F278_N279 insGG	15.74 ± 1.85	50.2	49.8	3.73 ± 0.54	92.7	4.9	2.4	3.49 ± 0.16	94.1	5.9
F278_N279 insGGG	13.44 ± 1.33	55.0	45.0	4.18 ± 0.37	93.3	2.7	4.0	2.48 ± 0.11	93.5	6.5
F278_N279 insGGGG	7.07 ± 1.56	40.4	59.6	3.87 ± 0.30	95.2	1.3	3.5	0.45 ± 0.08	92.3	7.7
F278_N279 insGGGGG	4.59 ± 0.46	55.4	44.6	1.58 ± 0.06	95.5	3.1	1.4	1.37 ± 0.06	92.5	7.5
F278_N279 insGGGGG G	20.69 ± 0.03	49.0	51.0	3.05 ± 0.05	95.7	2.4	2.0	2.31 ± 0.00	92.4	7.6
F278_N279 insGS	14.23 ± 0.67	42.5	57.5	3.45 ± 0.38	94.0	6.0	0.0	0.57 ± 0.04	93.0	7.0
F278_N279 insGSG	13.97 ± 0.33	33.2	66.8	1.60 ± 0.05	91.9	3.2	4.9	0.64 ± 0.04	93.3	6.7
F278_N279 insGSGS	15.41 ± 0.18	34.1	65.9	1.30 ± 0.16	92.5	4.0	3.5	0.39 ± 0.05	91.8	8.2
F278_N279 insGSGSG	20.31 ± 2.89	33.5	66.5	0.82 ± 0.17	94.1	4.4	1.5	0.39 ± 0.08	91.0	9.0
F278_N279 insGSGSGS	15.09 ± 2.03	36.4	63.6	0.90 ± 0.08	95.6	4.4	0.0	0.32 ± 0.04	91.0	9.0
F278_N279 insPA	9.04 ± 1.31	27.8	72.2	0.97 ± 0.04	90.2	6.3	3.6	1.60 ± 0.32	92.8	7.2
F278_N279 insPAP	11.29 ± 0.61	49.4	50.6	2.21 ± 0.03	92.1	4.6	3.3	2.86 ± 0.16	95.5	4.5
F278_N279 insPAPA	14.23 ± 0.54	52.9	47.1	3.66 ± 0.11	92.7	3.7	3.7	6.16 ± 0.14	96.0	4.0
F278_N279 insPAPAP	14.11 ± 1.25	15.8	84.2	6.03 ± 0.22	92.2	3.4	4.4	1.76 ± 0.01	94.0	6.0
F278_N279 insPAPAPA	9.82 ± 3.56	0.0	100.0	2.29 ± 0.19	92.5	3.5	4.0	0.73 ± 0.00	93.9	6.1
F278_N279 insGP	11.55 ± 0.73	58.2	41.8	1.21 ± 0.03	92.3	4.1	3.7	7.42 ± 0.00	95.6	4.4
F278_N279 insGPG	11.76 ± 1.59	29.4	70.6	6.92 ± 0.68	89.0	5.2	5.7	1.72 ± 0.06	93.5	6.5
F278_N279 insGPGP	13.71 ± 0.08	17.3	82.7	4.44 ± 0.12	87.6	6.8	5.6	1.31 ± 0.04	92.2	7.8
F278_N279 insGPGPG	13.31 ± 0.53	15.4	84.6	3.28 ± 0.19	87.6	3.6	8.8	1.02 ± 0.06	92.5	7.5
F278_N279 insGPGPGP	17.94 ± 1.41	11.6	88.4	2.37 ± 0.23	89.4	3.5	7.1	1.68 ± 0.05	92.2	7.8

Supplementary Table 8: Conversions of styrene 1, (*R*)-limonene 2 and 2-phenylpyridine 3 with the wild-type and insertion variants after Q286 based on LILI. Biotransformations were performed in technical triplicates and standard deviations (calculated using Excel version 2016) are indicated. Pf: combined product formation in mM. Regioselectivity in %. Source data are provided as a Source Data file.

	Pf (mM)	Selectivity (%)		Pf (mM)	Selectivity (%)			Pf (mM)	Selectivity (%)	
		1a	1b		2a	2b	2c		3a	3b
Wild-type	6.68 ± 0.77	86.4	13.6	3.58 ± 0.44	98.8	0.7	0.5	0.64 ± 0.03	93.0	7.0
Q286_A287 insGG	6.61 ± 0.70	11.2	88.8	0.45 ± 0.04	93.5	1.9	4.6	0.89 ± 0.02	83.6	16.4
Q286_A287 insGGG	8.74 ± 0.97	9.1	90.9	0.57 ± 0.05	91.2	3.6	5.2	1.38 ± 0.10	83.9	16.1
Q286_A287 insGGGG	0 ± 0	0.0	0.0	0 ± 0	0.0	0.0	0.0	0 ± 0	0.0	0.0
Q286_A287 insGGGGG	6.84 ± 1.08	6.2	93.8	0.23 ± 0.01	100.0	0.0	0.0	0.99 ± 0.03	85.4	14.6
Q286_A287 insGGGGG G	6.75 ± 0.26	7.1	92.9	0.19 ± 0.01	100.0	0.0	0.0	0.67 ± 0.04	86.1	13.9
Q286_A287 insGS	6.65 ± 2.69	0.0	100.0	0.48 ± 0.01	96.8	3.2	0.0	0.30 ± 0.01	84.9	15.1
Q286_A287 insGSG	15.00 ± 0.38	0.0	100.0	0.56 ± 0.05	100.0	0.0	0.0	0.36 ± 0.01	80.9	19.1
Q286_A287 insGSGS	0 ± 0	0.0	0.0	0 ± 0	0.0	0.0	0.0	0 ± 0	0.0	0.0
Q286_A287 insGSGSG	17.07 ± 1.03	0.0	100.0	0.25 ± 0.02	100.0	0.0	0.0	0.34 ± 0.01	83.4	16.6
Q286_A287 insGSGSGS	0 ± 0	0.0	0.0	0 ± 0	0.0	0.0	0.0	0 ± 0	0.0	0.0
Q286_A287 insPA	16.32 ± 1.13	30.2	69.8	1.87 ± 0.22	89.0	5.5	5.5	1.26 ± 0.08	86.4	13.6
Q286_A287 insPAP	19.14 ± 1.6	15.6	84.4	1.35 ± 0.08	89.1	5.4	5.5	1.34 ± 0.07	87.8	12.2
Q286_A287 insPAPA	15.10 ± 0.94	7.5	92.5	0.96 ± 0.04	89.5	4.2	6.3	1.01 ± 0.01	85.8	14.2
Q286_A287 insPAPAP	2.39 ± 0.50	12.2	87.8	0.88 ± 0.05	92.4	5.1	2.5	0.78 ± 0.03	91.2	8.8
Q286_A287 insPAPAPA	18.93 ± 1.19	7.1	92.9	0.73 ± 0.078	93.2	4.9	1.9	0.96 ± 0.02	89.6	10.4
Q286_A287 insGP	11.52 ± 0.79	11.8	88.2	0.66 ± 0.05	92.4	3.4	4.2	1.37 ± 0.07	86.0	14.0
Q286_A287 insGPG	13.35 ± 1.26	7.5	92.5	1.23 ± 0.08	95.6	2.4	2.0	1.86 ± 0.03	79.8	20.2
Q286_A287 insGPGP	13.94 ± 0.61	7.9	92.1	0.59 ± 0.05	91.1	3.7	5.1	1.23 ± 0.05	88.5	11.5
Q286_A287 insGPGPG	14.52 ± 0.61	5.8	94.2	0.86 ± 0.04	92.7	3.8	3.4	1.92 ± 0.08	81.4	18.6
Q286_A287 insGPGPGP	15.67 ± 0.24	6.5	93.5	0.42 ± 0.03	88.1	7.0	4.8	1.04 ± 0.01	89.5	10.5



Supplementary Fig. 11: Biotransformation results with variants derived from the LILI approach. a, Product formation and distribution of the products **1a** (red, bottom bars) and **1b** (blue, top bars) obtained during the biotransformation of **1** with the wild-type and variants of the LILI library. **b**, Product formation and distribution of the products **2a** (green, bottom bars), **2b** (blue, middle bars) and **2c** (orange, top bars) obtained during the biotransformation of **2** with the wild-type and variants of the LILI library. **c**, Product formation and distribution of the products **3a** (green, bottom bars) and **3b** (purple, top bars) obtained during the biotransformation of **3** with the wild-type and variants of the LILI library. The reaction conditions as mentioned in Fig. 2 were applied, the substrate concentrations are indicated in the reaction equation. The reactions were performed in technical triplicates (black dots) with average values (horizontal bar) and standard deviations (calculated using Excel version 2016) indicated. Error bars may be covered by markers. Source data are provided as a Source Data file.

Supplementary Table 9: Different wild-types and active-site variants known from literature compared to selected loop variants from this study. t.w.: this work. n.d.: not determined. Source data are provided as a Source Data file.

		Product formation (%)	Selectivity (%)			Annotation	Source		
			1a	1b					
Styrene 1	CDO wild-type	13.4 ± 1.55	86.4	13.6 (ee 18.4 ± 1.1 R-1b)		50 mM substrate 0.1 g _{cww} /ml <i>E. coli</i>	t.w.		
	Literature	CDO wild-type (<i>Pseudomonas fluorescens</i> IP01)	71 ± 6	99.7	0.3 (ee 43 ± 3 R-1b)		10 mM substrate, 0.2 g _{cww} /ml <i>E. coli</i>	1	
		NDO wild-type (<i>Pseudomonas</i> sp. NCIB 9816-4)	74 ± 3	0	>99 (ee 78 ± 1 R-1b)		10 mM substrate, 0.2 g _{cww} /ml <i>E. coli</i>	2	
		TDO wild-type (<i>Pseudomonas. putida</i> F1)	9	85	15 (ee >99 R-1b)		10 mM substrate	3	
	Active-site	CDO_M232A	97 ± 10	8	92 (ee 95 ± 1 R-1b)		10 mM substrate, 0.2 g _{cww} /ml <i>E. coli</i>	1	
		NDO_H295A	92 ± 2	<1	>99 (ee 79 ± 1 R-1b)		10 mM substrate, 0.2 g _{cww} /ml <i>E. coli</i>	2	
		TDO_T365N	14	24	76 (ee >99 R-1b)		10 mM substrate,	3	
	Loop	CDO_N279_D280insE	47.4 ± 3.2	67.5	32.5 (ee 11.4 ± 5.8 R-1b)		50 mM substrate 0.1 g _{cww} /ml <i>E. coli</i>	t.w.	
		CDO_F282A	24.6 ± 5.7	95.0	5.0 (ee 72.7 ± 0.6 R-1b)		50 mM substrate 0.1 g _{cww} /ml <i>E. coli</i>	t.w.	
		CDO_Q286_A287insGSGSG	34.1 ± 2.1	<1	>99 (ee 6.4 ± 0.2 R-1b)		50 mM substrate 0.1 g _{cww} /ml <i>E. coli</i>	t.w.	
		CDO_F282_L284del	39.9 ± 4.0	6.3	93.7 (ee 1.4 ± 0.6 R-1b)		50 mM substrate 0.1 g _{cww} /ml <i>E. coli</i>	t.w.	
				2a	2b	2c			
	(R)-Limonene 2	CDO wild-type	35.8 ± 4.4	98.8 (ee 99.6 ± 0.1 1R,5S-2a)	0.7	0.5	0.1 g _{cww} /ml <i>E. coli</i>	t.w.	
		Literature	CDO wild-type (<i>Pseudomonas fluorescens</i> IP01)	46 ± 10	> 95 (ee > 98 ± 0.1 1R,5S-2a)	<5	0	0.2 g _{cww} /ml <i>E. coli</i>	1
			CDO wild-type (<i>Pseudomonas putida</i> S1)	40	>95 (ee >98 1R,5S-2a)	0	0	OD ₆₀₀ = 3.0 6.2 mM substrate	4
			NDO wild-type (<i>Pseudomonas</i> sp. NCIB 9816-4)	n.d.	92	8	0	0.2 g _{cww} /ml <i>E. coli</i>	2
Active-site		CDO_M232A	>99	95 (ee > 98 1R,5S-2a)	5	0	0.2 g _{cww} /ml <i>E. coli</i>	1	
		NDO_H295A_V260A	213% of wild-type	93 (ee 62 1R,5S-2a)	7	0	0.2 g _{cww} /ml <i>E. coli</i>	2	
Loop		CDO_A283del	89.2 ± 8.0	98.2 (ee 62 1R,5S-2a)	0.8	1.0	0.1 g _{cww} /ml <i>E. coli</i>	t.w.	
		CDO_L284G	20.8 ± 1.9	30.8 (ee >99 1R,5S-2a)	19.4	49.7	0.1 g _{cww} /ml <i>E. coli</i>	t.w.	
		CDO_M289A	19.4 ± 0.9	54.1 (ee >99 1R,5S-2a)	6.2	39.8	0.1 g _{cww} /ml <i>E. coli</i>	t.w.	

			3a	3b			
2-Phenylpyridine 3	CDO wild-type	6.4 ± 0.3	93.0 (<i>ee</i> >99 1 <i>S</i> , 2 <i>R</i> -3a)	7.0		t.w.	
	Literature	TDO wild-type (<i>Pseudomonas putida</i> UV4)	1% yield	100 (<i>ee</i> >98 1 <i>S</i> , 2 <i>R</i> -3a)			5
		NDO wild-type (<i>Pseudomonas</i> sp. NCIB 9816-4)	25% yield	≥95		≤5% <i>cis</i> -3,4- dihydrodiol (<i>ee</i> >98 1 <i>S</i> , 2 <i>R</i>) was formed	5
		BPDO wild-type (<i>Sphingomonas yanoikuyae</i> (B8/36))	59% yield	≥95			5
	Loop	CDO_A283del	>99	98.7 (<i>ee</i> >99 1 <i>S</i> , 2 <i>R</i> -3a)	1.3		t.w.
		CDO_F282A	99.9 ± 4.0	98.6 (<i>ee</i> >99 1 <i>S</i> , 2 <i>R</i> -3a)	1.4		t.w.
		CDO_Q286_A287insGPG	18.6 ± 0.3	79.8 (<i>ee</i> >99 1 <i>S</i> , 2 <i>R</i> -3a)	20.2		t.w.

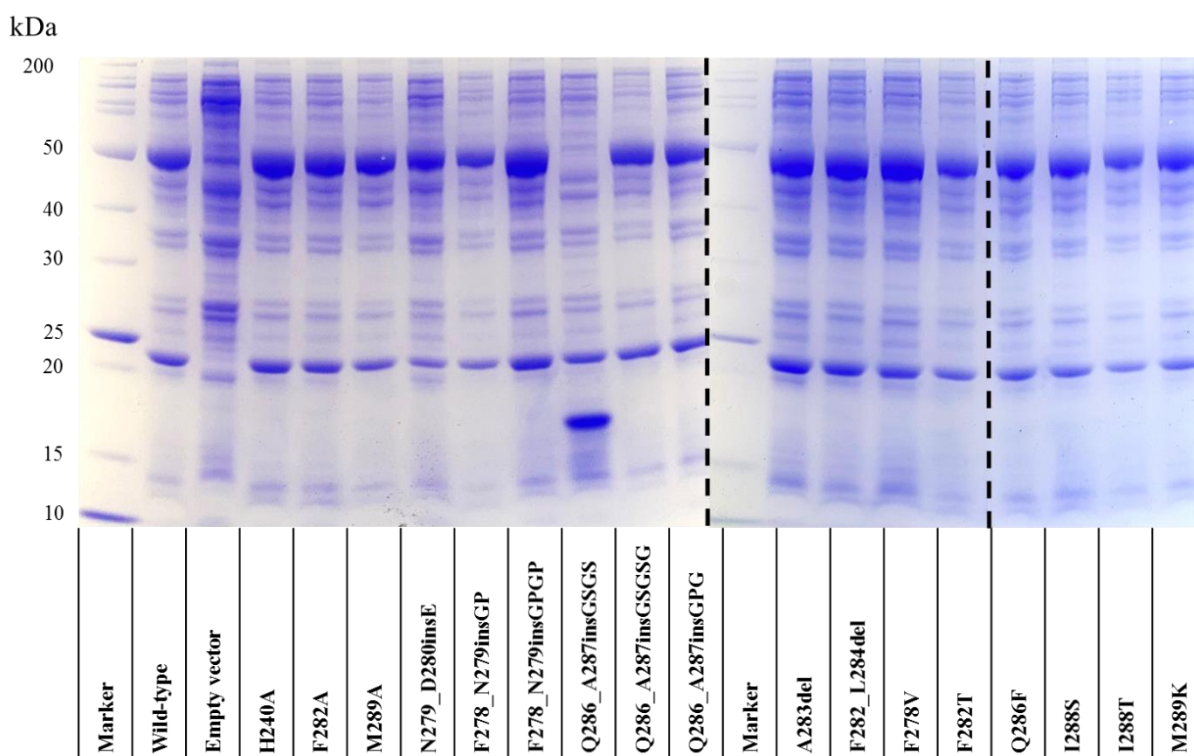
Supplementary Table 10: Enantiomeric excesses of the biotransformations of styrene 1, (*R*)-limonene 2 and 2-phenylpyridine 3 with the selected variants from Supplementary Table S19, and saturation and deletion variants. Biotransformations were performed in technical triplicates and standard deviations (calculated using Excel version 2016) are indicated. Enantiomeric excess in %. n.d.: not determined. -: not detected. Source data are provided as a Source Data file.

Variant	Product (%)		
	Phenylethan-1,2-diol	Carveol	1,2-Dihydroxy-3-(2'-pyridyl)- cyclohexa-3,5-diene
	1b	2a	3a
Wild-type	18.43 ± 1.08 (<i>R</i>)-1b	99.73 ± 0.13 (1 <i>R</i> ,5 <i>S</i>)-2a	>99 % (+)-(1 <i>S</i> ,2 <i>R</i>)-3a
F282A	72.72 ± 0.63 (<i>R</i>)-1b	n.d.	>99 % (+)-(1 <i>S</i> ,2 <i>R</i>)-3a
M289A	n.d.	99.97 ± 0.05 (1 <i>R</i> ,5 <i>S</i>)-2a	>99 % (+)-(1 <i>S</i> ,2 <i>R</i>)-3a
N279_D280insE	11.42 ± 5.84 (<i>R</i>)-1b	n.d.	>99 % (+)-(1 <i>S</i> ,2 <i>R</i>)-3a
A283del	42.00 ± 0.59 (<i>R</i>)-1b	>99.9 (1 <i>R</i> ,5 <i>S</i>)-2a	>99 % (+)-(1 <i>S</i> ,2 <i>R</i>)-3a
F282_L284del	1.49 ± 0.15 (<i>R</i>)-1b	93.30 ± 0.72 (1 <i>R</i> ,5 <i>S</i>)-2a	>99 % (+)-(1 <i>S</i> ,2 <i>R</i>)-3a
F278V	41.32 ± 6.64 (<i>R</i>)-1b	99.99 ± 0.01 (1 <i>R</i> ,5 <i>S</i>)-2a	>99 % (+)-(1 <i>S</i> ,2 <i>R</i>)-3a
F282V	69.83 ± 3.61 (<i>R</i>)-1b	>99.9 (1 <i>R</i> ,5 <i>S</i>)-2a	>99 % (+)-(1 <i>S</i> ,2 <i>R</i>)-3a
F282T	-	>99.9 (1 <i>R</i> ,5 <i>S</i>)-2a	>99 % (+)-(1 <i>S</i> ,2 <i>R</i>)-3a
L284G	26.03 ± 1.08 (<i>R</i>)-1b	>99.9 (1 <i>R</i> ,5 <i>S</i>)-2a	>99 % (+)-(1 <i>S</i> ,2 <i>R</i>)-3a
Q286F	15.83 ± 0.23 (<i>R</i>)-1b	>99.9 (1 <i>R</i> ,5 <i>S</i>)-2a	>99 % (+)-(1 <i>S</i> ,2 <i>R</i>)-3a
I288S	15.56 ± 0.70 (<i>S</i>)-1b	99.76 ± 0.02 (1 <i>R</i> ,5 <i>S</i>)-2a	>99 % (+)-(1 <i>S</i> ,2 <i>R</i>)-3a
I288T	1.17 ± 0.83 (<i>S</i>)-1b	>99.9 (1 <i>R</i> ,5 <i>S</i>)-2a	>99 % (+)-(1 <i>S</i> ,2 <i>R</i>)-3a
M289K	23.97 ± 0.44 (<i>R</i>)-1b	>99.9 (1 <i>R</i> ,5 <i>S</i>)-2a	>99 % (+)-(1 <i>S</i> ,2 <i>R</i>)-3a

The enantiomeric excess of 3a was determined by comparison to two in-house standards of (+)-(1*S*,2*R*)-3a. The configuration was determined by optical rotation.⁵ Multiple columns and methods were applied, which all reveal only one enantiomer.

Supplementary Table 11: Diastereomeric excesses of the biotransformations (*R*)-limonene 2 with the selected variants from Supplementary Table 10, saturation and deletion variants. Biotransformations were performed in technical triplicates and standard deviations (calculated using Excel version 2016) are indicated. Diastereomeric excess in %. Source data are provided as a Source Data file.

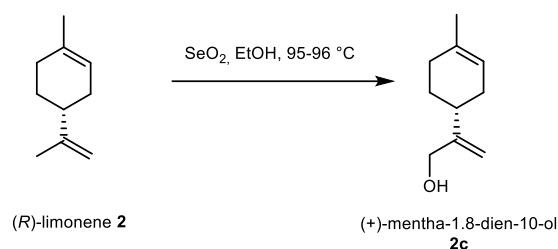
Variant	Carveol 2a
Wild-type	94.70 ± 0.37 (1 <i>R</i> ,5 <i>S</i>)-2a
M289A	97.05 ± 0.26 (1 <i>R</i> ,5 <i>S</i>)-2a
A283del	87.27 ± 1.14 (1 <i>R</i> ,5 <i>S</i>)-2a
F282_L284del	98.41 ± 0.02 (1 <i>R</i> ,5 <i>S</i>)-2a
F278V	55.10 ± 2.53 (1 <i>R</i> ,5 <i>S</i>)-2a
F282V	99.14 ± 0.01 (1 <i>R</i> ,5 <i>S</i>)-2a
F282T	99.41 ± 0.20 (1 <i>R</i> ,5 <i>S</i>)-2a
L284G	38.14 ± 1.81 (1 <i>R</i> ,5 <i>S</i>)-2a
Q286F	98.11 ± 0.08 (1 <i>R</i> ,5 <i>S</i>)-2a
I288S	90.23 ± 1.53 (1 <i>R</i> ,5 <i>S</i>)-2a
I288T	99.12 ± 0.06 (1 <i>R</i> ,5 <i>S</i>)-2a
M289K	88.02 ± 0.82 (1 <i>R</i> ,5 <i>S</i>)-2a



Supplementary Fig. 12: SDS-PAGE analysis of the empty vector, expressed wild-type and selected variants of the CDO. The analysis of the expression levels was performed in a RunBlue 12% Bis-Tris Gel from Expedeon (Abcam, Berlin, Germany) with PageRuler™ Unstained Protein Ladder (Thermo Scientific, Waltham, USA) as marker. Whole cell samples were standardized to $OD_{600} = 4$. The bands of the α -subunit (52 kDa) and β -subunit (23 kDa) are clearly visible, except for the α -subunit of Q286_A287insGSGS. The bands of the reductase (44 kDa) and ferredoxin (12 kDa) were not observed. Source data are provided as a Source Data file. Dashed lines represent different gels and vertically sliced image. SDS-PAGE analysis was performed independently 15 times for the wildtype with comparable results. Other variants were analyzed *via* SDS-PAGE with the wildtype as positive control at least once and repeated when preparation errors occurred.

All obtained variants were analyzed *via* non-native SDS-PAGE of the whole cells as shown in Supplementary Fig. S12. All variants, also these which showed no activity for any of the tested variants, were expressed. No native SDS-PAGE was observed, so no conclusions about the solubility or correct folding could be drawn.

Supplementary Note 1: Synthesis of (+)-mentha-1.8-dien-10-ol (2b)

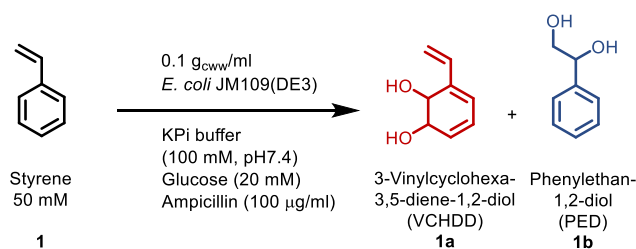


The synthesis of (+)-mentha-1.8-dien-10-ol **2b** was performed according to Thomas and Bucher.⁶

Yellow oil; ¹H NMR (500 MHz, CDCl₃): δ 1.43-1.56 (2 H, m), 1.66 (3 H, s), 1.78-2.23 (6 H, m), 4.18 (2 H, d, *J* 5.7), 4.91 (1 H, s), 5.04-5.07 (1 H, m), 5.40 (1 H, br s); ¹³C NMR (500 MHz CDCl₃): δ 23.48, 28.18, 30.53, 31.36, 36.91, 65.19, 107.83, 120.45, 133.85, 153.67. MS (GC, ED): *m/z* (%) = 153 (1, M⁺), 152 (11.8, M), 134 (47), 121 (17), 119 (91), 107 (14), 106 (100), 105 (39), 94 (34), 93 (61), 92 (46), 91 (82), 84 (25), 83 (16), 79 (80), 77 (42), 68 (60), 67 (72), 65 (16)

GC-MS and NMR analysis revealed contaminations with formed perillyl alcohol.

Supplementary Note 2: Determination of product formation, distribution, enantiomeric excess and diastereomeric excess



Supplementary Fig. 13: Conversion of styrene to 3-vinylcyclohexa-3,5-diene-1,2-diol **1a** and 1-phenylethan-1,2-diol **1b**

3-vinylcyclohexa-3,5-diene-1,2-diol (1a)

MS (GC, EI) m/z (%) = 139 (1.7, M⁺), 138 (19, M), 120 (94), 109 (21), 92 (39), 91 (100), 81 (19), 79 (23), 77 (24), 65 (17)

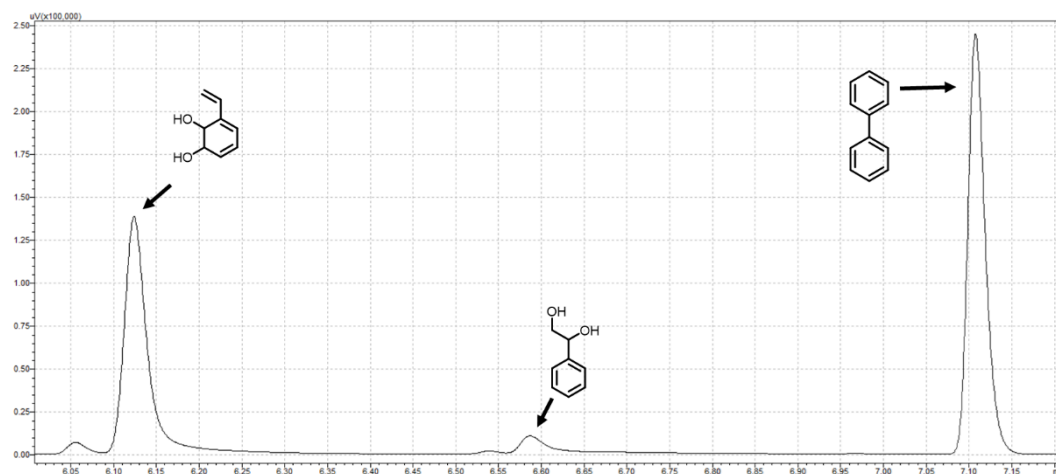
1-phenyl-1,2-ethanediol (1b)

Rieske non-heme iron oxygenase (RO)-catalyzed biotransformations

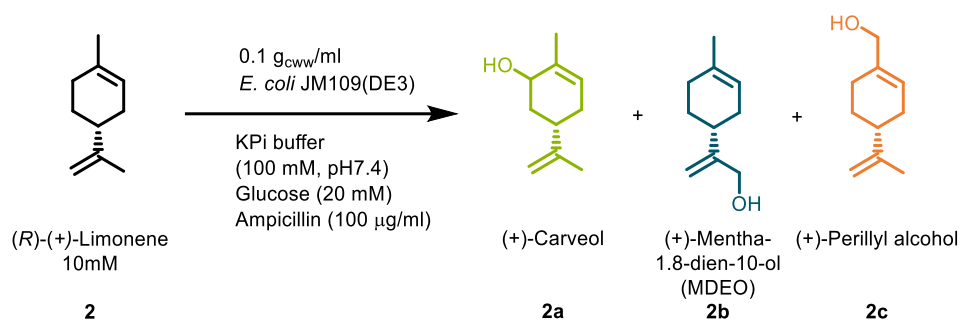
MS (GC, EI) m/z (%) = 139 (0.8, M⁺), 138 (9, M), 108 (9), 107 (100), 91 (4), 79 (48), 77 (28)

Standard Sigma Aldrich

MS (GC, EI) m/z (%) = 139 (2, M⁺), 138 (23, M), 108 (22), 107 (100), 91 (10), 79 (100), 77 (77)



Supplementary Fig. 14: GC-FID chromatogram of CDO wild-type catalyzed biotransformation of styrene 1.



Supplementary Fig. 15: Conversion of (R)-(+)-limonene 2 to (+)-carveol 2a, (+)-mentha-1.8-dien-10-ol 2b and (+)-perillyl alcohol 2c.

(+)-carveol 2a

Rieske non-heme iron oxygenase (RO)-catalyzed biotransformation

MS (GC, EI) m/z (%) = 153 (1.2, M⁺), 152 (11, M), 137 (11), 119 (11), 109 (100), 108 (13), 95 (13), 94 (4), 93 (11), 92 (5), 91 (15), 84 (47), 83 (25), 81 (10), 80 (8), 79 (10), 69 (17), 55 (18)

Standard Sigma-Aldrich

MS (GC, EI) m/z (%) = 153 (0.3, M⁺), 152 (3, M), 137 (68), 119 (34), 109 (77), 108 (12), 95 (24), 94 (25), 93 (27), 92 (17), 91 (24), 84 (100), 83 (44), 81 (25), 80 (25), 79 (24), 69 (36), 55 (31)

(+)-mentha-1.8-dien-10-ol 2b

Rieske non-heme iron oxygenase (RO)-catalyzed biotransformation

MS (GC, EI) m/z (%) = 153 (5, M⁺), 152 (18, M), 134 (63), 121 (27), 119 (100), 107 (22), 106 (79), 105 (50), 95 (29), 94 (49), 93 (80), 92 (54), 91 (82), 84 (40), 79 (95), 77 (42), 68 (95), 67 (98), 55 (49)

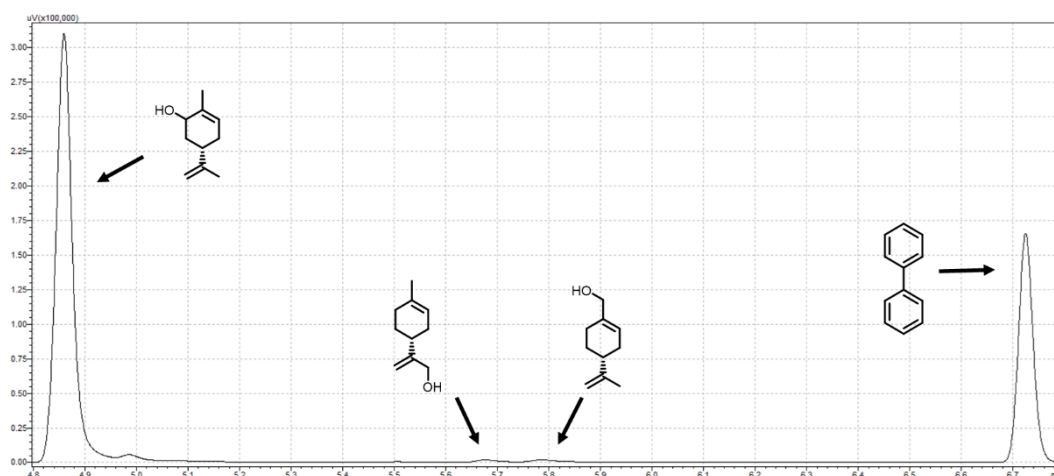
(+)-perillyl alcohol 2c

Rieske non-heme iron oxygenase (RO)-catalyzed biotransformation

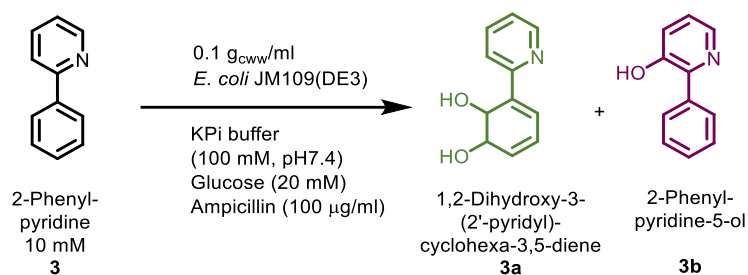
MS (GC, EI) m/z (%) = 153 (1.6, M⁺), 152 (9, M), 121 (83), 119 (31), 109 (26), 108 (28), 107 (37), 106 (18), 105 (22), 95 (38), 94 (52), 93 (95), 91 (53), 81 (37), 79 (100), 77 (30), 68 (90), 67 (80), 55 (44)

Standard Sigma-Aldrich

MS (GC, EI) m/z (%) = 153 (2, M^+), 152 (18, M), 121 (87), 119 (48), 109 (35), 108 (33), 107 (14), 106 (28), 105 (28), 95 (18), 94 (18), 93 (90), 91 (61), 81 (29), 79 (100), 77 (32), 68 (86), 67 (77), 55 (39)



Supplementary Fig. 16: GC-FID chromatogram of CDO wild-type catalyzed biotransformation of (*R*)-(+)-limonene 2.



Supplementary Fig. 17: Conversion of 2-phenylpyridine 3 to 1,2-dihydroxy-3-(2'-pyridyl)-cyclohexa-3,5-diene 3a and 2-phenylpyridine-5-ol 3b.

1,2-dihydroxy-3-(2'-pyridyl)-cyclohexa-3,5-diene 3a

Rieske non-heme iron oxygenase (RO)-catalyzed biotransformations

MS (LC, ESI, positive) m/z (%) = 191 (M⁺, 12), 190 (100, M), 189 (58), 173 (4), 172 (35)

Standard from in-house library, derived from an upscaling of biotransformation of 2-phenylpyridine with TDO Wild-type

MS (LC, ESI, positive) m/z (%) = 191 (M⁺, 6), 190 (100, M), 173 (6), 172 (48)

Brown solid; $[\alpha]_D^{+161}$ (c 1.1, MeOH); ¹H NMR δ (CDCl₃, 500 MHz), 4.50 (1 H, m, H-1), 4.93 (1 H, d, $J_{1,2}$ 9.7, H-2), 6.18 (2 H, m, H-5, H-6), 6.65 (1 H, d, $J_{4,5}$ 5.4, H-4), 6.89 (1 H, dd, $J_{4',3'}$ 9.9, $J_{4',5'}$ 2.5, H-4'), 7.51 (1 H, d, $J_{3',4'}$ 5.4, H-3'), 7.6 (1 H, d, $J_{5',4'}$ 8, H-5'), 8.51 (1 H, d, $J_{6',5'}$ 4.6, H-6'); ¹³C NMR δ (500 MHz, CDCl₃) 67.26, 69.24, 119.98, 122.13, 123.58, 124.82, 131.44, 136.21, 136.97, 148.19, 157.33; ⁵

2-phenylpyridine-5-ol 3b

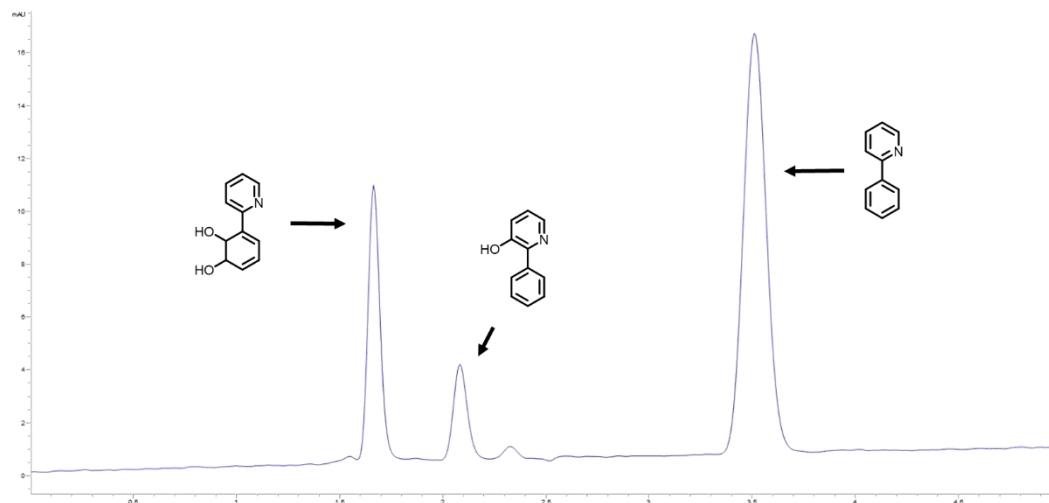
Rieske non-heme iron oxygenase (RO)-catalyzed biotransformations

MS (LC, ESI, positive) m/z (%) = 173 (12, M⁺), 172 (100, M)

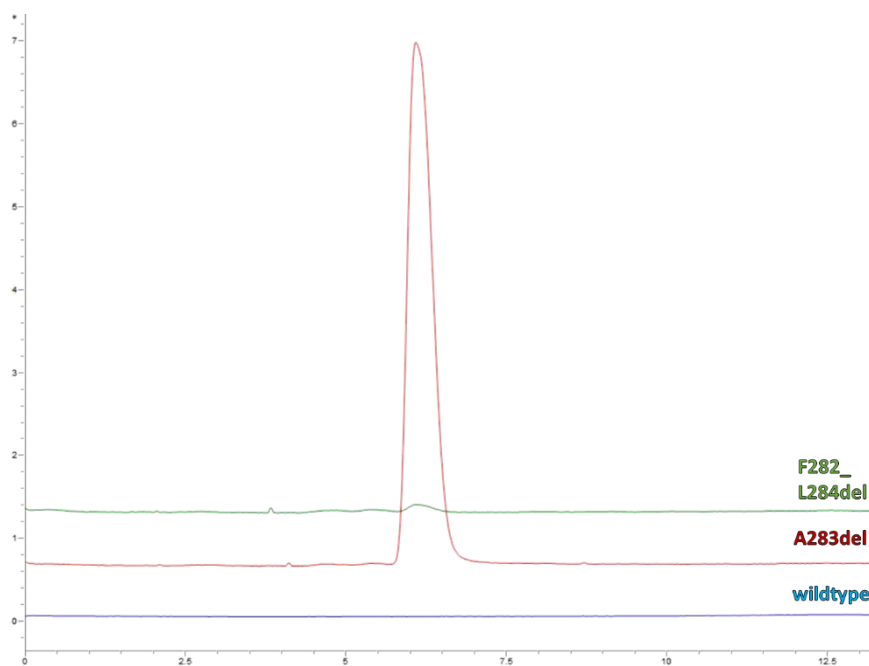
Standard Fluorochem

MS (LC, ESI, positive) m/z (%) = 173 (13, M⁺), 172 (100, M)

MS (GC, EI) m/z (%) = 172 (5.6, M⁺), 171 (52, M), 170 (100), 169 (2), 144 (1), 143 (7), 142 (7), 141 (3), 140 (2), 117 (6), 116 (9), 115 (27)



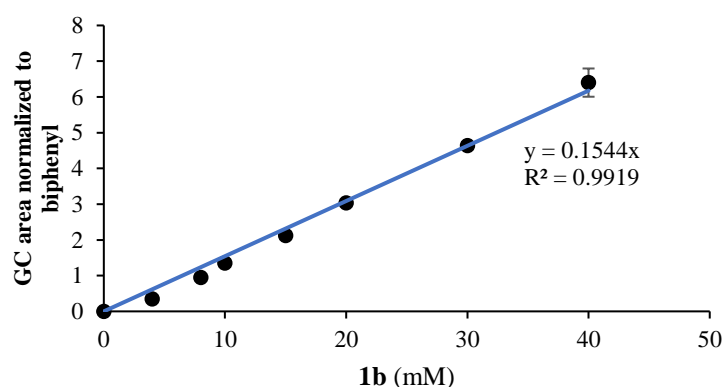
Supplementary Fig. 18: DAD chromatogram of CDO wild-type catalyzed biotransformation of 2-phenylpyridine at a wavelength of 210 nm.



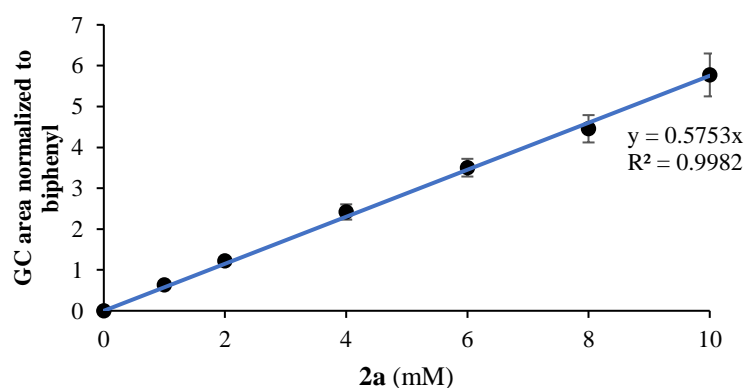
Supplementary Fig. 19: LC-MS spectrum of the biotransformation of phenazone in SIM-mode (m/z 222). Comparison between the wild-type (blue, bottom line) with no product formation, F282_L284del (green, top line) with product traces and A283del (red, middle line) with clear product formation.

Product formations and distribution

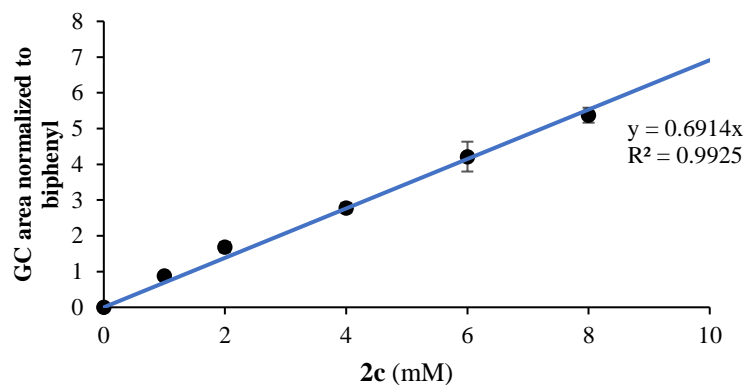
The quantification of the different products was performed with biphenyl as internal standard under the same conditions as the corresponding biotransformations. 1 M DMSO stocks of the corresponding products were applied for standard solutions, incubated, extracted and analyzed. LC/MS analysis of the in-house standard of 1,2-dihydroxy-3-(2'-pyridyl)-cyclohexa-3,5-diene (**3a**) showed traces of 2-phenyl-pyridine-5-ol (**3b**). Based on the corresponding calibration curve, the amount of 2-phenyl-pyridine-5-ol was subtracted from the used concentration of 1,2-dihydroxy-3-(2'-pyridyl)-cyclohexa-3,5-diene standard to ensure correct concentrations.



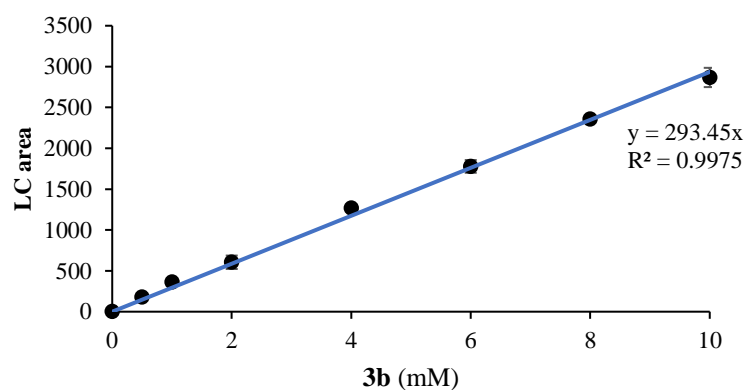
Supplementary Fig. 20. Calibration curve of 1-phenyl-1,2-ethandiol (1b). Data acquisition was performed in technical triplicates per concentration with average values and standard deviations (calculated using Excel version 2016) are indicated. Error bars may be covered by markers. Source data are provided as a Source Data file.



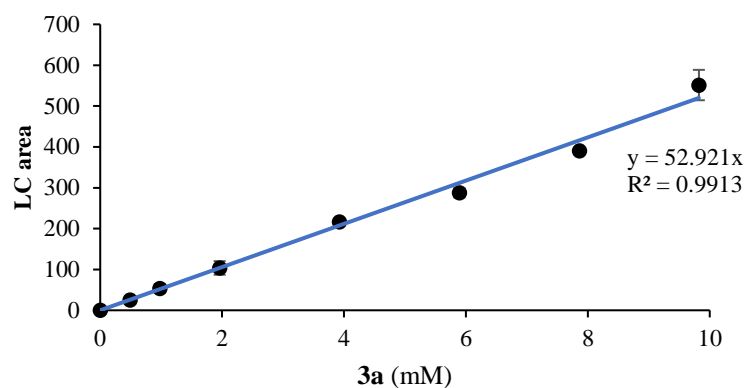
Supplementary Fig. 21. Calibration curve of the mixture of isomers of (-)-carveol (2a). Data acquisition was performed in technical triplicates per concentration with average values and standard deviations (calculated using Excel version 2016) are indicated. Error bars may be covered by markers. Source data are provided as a Source Data file.



Supplementary Fig. 22. Calibration curve of (+)-perillyl alcohol (2c). Data acquisition was performed in technical triplicates per concentration with average values and standard deviations (calculated using Excel version 2016) are indicated. Error bars may be covered by markers. Source data are provided as a Source Data file.



Supplementary Fig. 23. Calibration curve of 2-phenyl-pyridine-5-ol (3b). Data acquisition was performed in technical triplicates per concentration with average values and standard deviations (calculated using Excel version 2016) are indicated. Error bars may be covered by markers. Source data are provided as a Source Data file.



Supplementary Fig. 24. Calibration curve of 1,2-dihydroxy-3-(2'-pyridyl)-cyclohexa-3,5-diene (3a). Data acquisition was performed in technical triplicates per concentration with average values and standard deviations (calculated using Excel version 2016) are indicated. Error bars may be covered by markers. Source data are provided as a Source Data file.

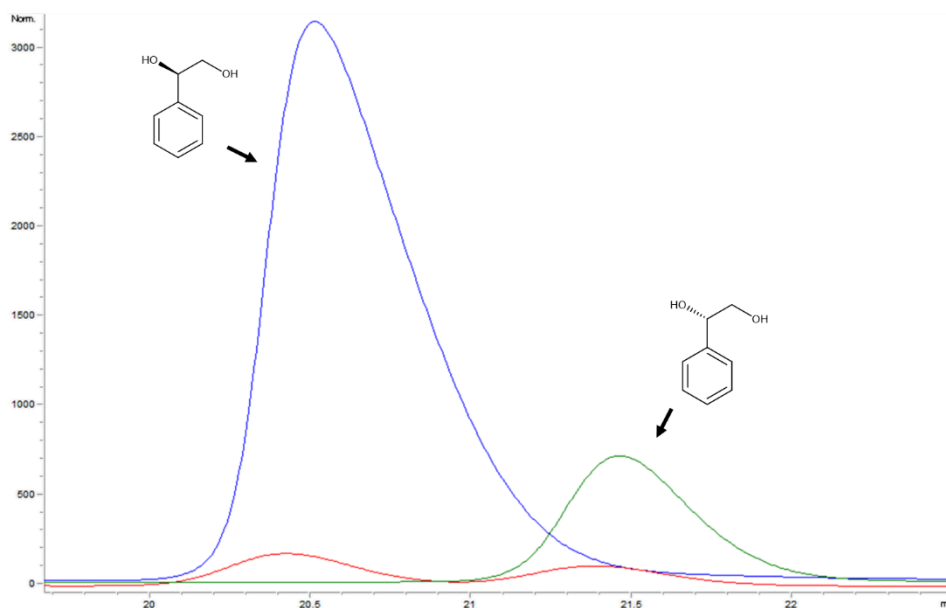
The product 3-vinylcyclohexa-3,5-diene-1,2-diol **1a** polymerizes when concentrated in vacuo, so the synthesis of a standard for quantification is not possible. Also, the synthesis of (+)-mentha-1.8-dien-10-ol **2b** yielded a standard with impurities with perillyl alcohol, despite repeated column chromatography. To ensure correct quantification, we used the relative response factor to determine the concentrations in reference to a standard.^{7,8} For **1a**, we used **1b** as standard, while **2c** was applied as reference standard for **2b**. The RF values were calculated from the effective carbon numbers (ECN) of the respective compound (ECN_X) in relation the the ECN of the standard (ECN_{STD}) with equation (1).

$$RF = \frac{ECN_X}{ECN_{STD}} \quad (1)$$

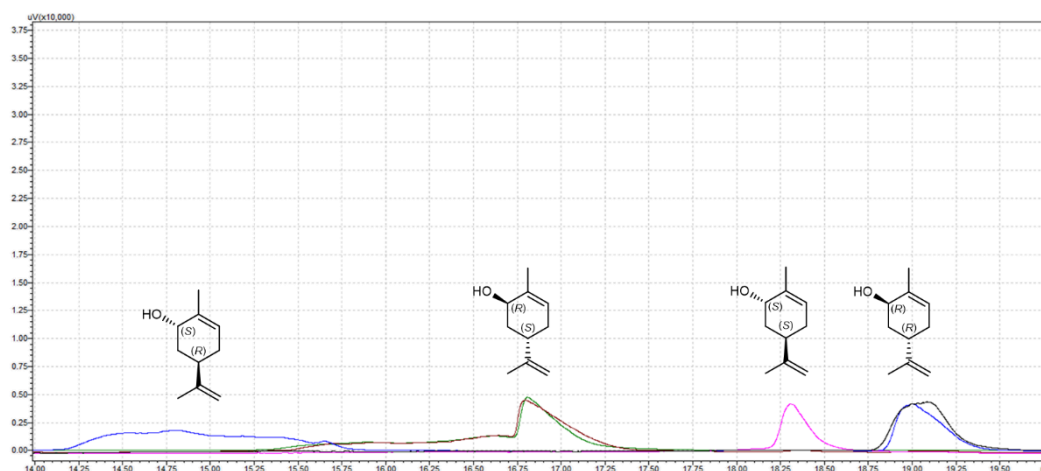
Calibration curves were determined by the quantification of the analytes by external calibration and normalization by the calculated RF values (Supplementary Table 12).

Supplementary Table 12: Calculated ECN and RF values.

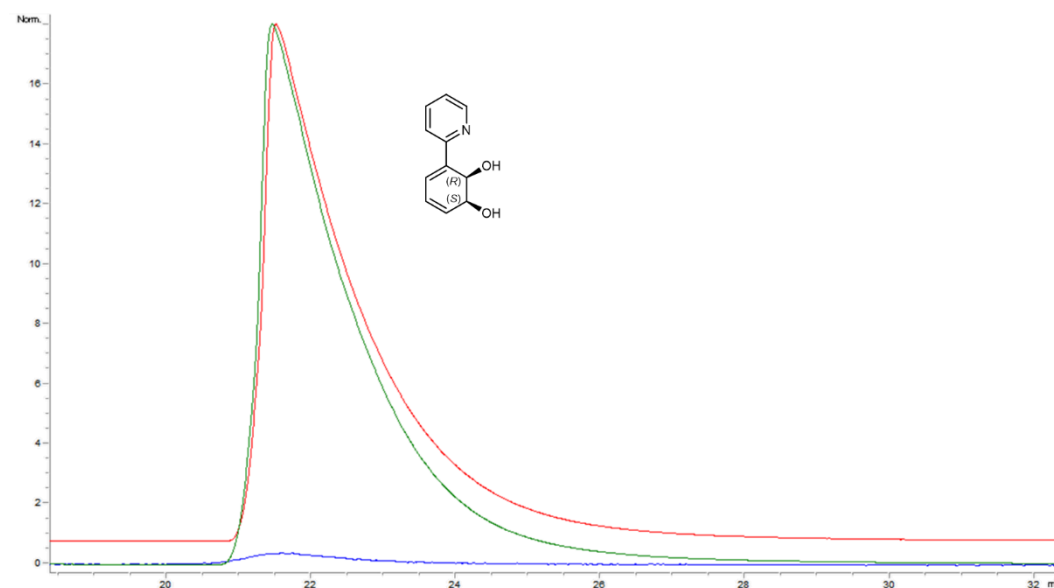
Compound	ECN	RF
1a	6.2	0.919
1b	6.5	
2b	9.3	1
2c	9.3	



Supplementary Fig. 25: Chiral HPLC analysis of 1-phenyl-1,2-ethandiol 1b enantiomers of the commercially available standards of (*R*)-1b (blue, Sigma Aldrich, 99 % optical purity), (*S*)-1b (green, Sigma Aldrich, 99 % optical purity) and the RO-catalyzed biotransformation of 1 (red).

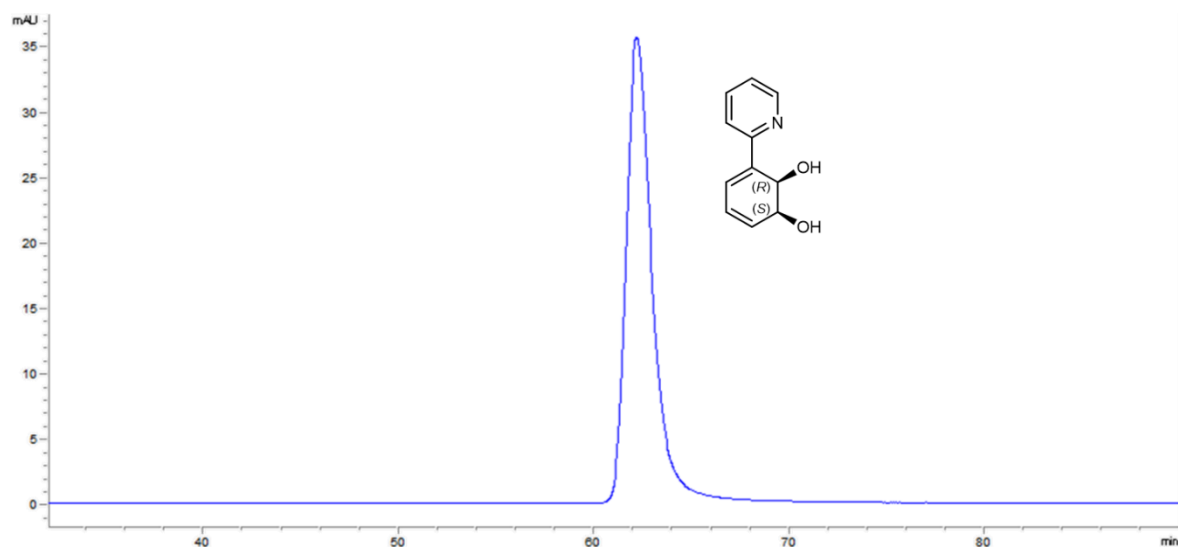


Supplementary Fig. 26: Chiral GC-FID analysis of carveol 2a enantiomers. Commercially available isomer mixture of (-)-carveol (black, Sigma Aldrich, 97 %) containing (1*S*,5*R*)-**2a** and (1*R*,5*R*)-**2a**. (1*S*,5*S*)-carveol (pink) from our in-house library, synthesis according to Bermejo *et al.*^{1,9} (1*R*,5*R*)-carveol (blue) from our in-house library, synthesis according to Dhulut *et al.*^{1,10} (1*R*,5*S*)-carveol (green) derived from CDO_M232A-catalyzed biotransformation of **1**.¹ (1*R*,5*S*)-carveol (red) derived from CDO wild-type-catalyzed biotransformation of **1**.



Supplementary Fig. 27: Chiral HPLC analysis of (1*S*,2*R*)-1,2-dihydroxy-3-(2'-pyridyl)-cyclohexa-3,5-diene **3a with normal phase CHIRALPAK IB column. CDO wild-type (blue) and CDO_A283del (red) catalyzed biotransformation of **3**. In-house standard of (1*S*,2*R*)-**3a** (green).**

We also evaluated a normal phase CHIRALPAK IC (250 mm x 4.6 mm, 5 μ m particle size, Daicel (Europa) GmbH, Raunheim, Germany) for additional enantiomers of (1*S*,2*R*)-1,2-dihydroxy-3-(2'-pyridyl)-cyclohexa-3,5-diene. 6 μ l sample were injected and the compounds were separated with 1.4 ml/min isocratic mobile phase of 90:10 n-hexane/isopropanol at 30 $^{\circ}$ C on the same normal phase HPLC-DAD system mentioned in the methods section. Analysis was performed using the DAD at a wavelength of 310 nm. Despite a length of 90 min and previously successful separation of enantiomers of similar products with this column, no additional peak was observed.



Supplementary Fig. 28: Chiral HPLC analysis of (1*S*,2*R*)-1,2-dihydroxy-3-(2'-pyridyl)-cyclohexa-3,5-diene **3a with normal phase CHIRALPAK IC column. CDO wild-type (blue) and CDO_A283del (red) catalyzed biotransformation of **3**. In-house standard of (1*S*,2*R*)-**3a** (green).**

Primers

Supplementary Table 13: Sequencing primers used in this study.

Name	Sequence (5' → 3')
pIP107D_seq1f	GATATGTACCATGCGGG
pIP107D_seq2f	CCAAAATGTACAGCTGTG
pIP107D_seq3f	GTGGATTTGCAGGTCGG
pIP107D_seq4f	GCCGCTGAAGATATATCCG
pIP107D_seq5f	GGTATCGCATGTGAGC

Supplementary Table 14: Site-directed mutagenesis primers used for the alanine scan.

Mutation	Name	Sequence (5' → 3')
G236A	G236A_fw	GATATGTACCATGCGGCAACGATGGCGCATCTT
	G236A_rv	GCGCCATCGTTGCCGCATGGTACATATC
T237A	T237A_fw	GCGGGAGCGATGGCGCATCTTTC
	T237A_rv	GAAAGATGCGCCATCGCTCCCGC
M238A	M238A_fw	GTACCATGCGGGAACGGCGGCATCTTTCAGGT
	M238A_rv	ACCTGAAAGATGCGCCCGCTTCCCGCATGGTAC
A239G	A239G_fw	GGAACGATGGGCCATCTTTCAG
	A239G_rv	CTGAAAGATGGCCCATCGTTCC
H240A	H240A_fw	CATGCGGGAACGATGGCGGCTCTTTCAGGTGTATTGTC
	H240A_rv	GACAATACACCTGAAAGAGCCGCATCGTTCCCGCATG
L241A	L241A_fw	GGACAATACACCTGAAGCATGCGCCATCGTTCCCG
	L241A_rv	CGGGAACGATGGCGCATGCTTCAGGTGTATTGTCC
D242A	D242A_fw	GGGAACGATGGCGCATCTTTCAGGTGTATTGTCCAGCCTCCCG
	D242A_rv	AAGATGCGCCATCGTTCCCGCATGGTACATATCGCTACAGAATTG
G243G	G243G_fw	GAACGATGGCGCATCTTTCAGCTGTATTGTCCAGCCTCCCGCC
	G243G_rv	CTGAAAGATGCGCCATCGTTCCCGCATGGTACATATCGCTACAGAAT
V244A	V244A_fw	GATGGCGCATCTTTCAGGTGCATTGTCCAGCCTCCCGCC
	V244A_rv	CACCTGAAAGATGCGCCATCGTTCCCGCATGGTACATATCGC
L245A	L245A_fw	GATGGCGCATCTTTCAGGTGTAGCGTCCAGCCTCCCGCCTG
	L245A_rv	TACACCTGAAAGATGCGCCATCGTTCCCGCATGGTACATATCGC
S246A	S246A_fw	GCGCATCTTTCAGGTGTATTGGCCAGCCTCCCGCCTGAAATG
	S246A_rv	CAATACACCTGAAAGATGCGCCATCGTTCCCGCATGGTACATATCG
S247A	S247A_fw	GCATCTTTCAGGTGTATTGTCCGCCCTCCCGCCTGAAATGGATTGTC
	S247A_rv	GGACAATACACCTGAAAGATGCGCCATCGTTCCCGCATGGTAC
L248A	L248A_fw	GGTGTATTGTCCAGCGCCCCGCCTGAAATGGATT
	L248A_rv	AATCCATTTTCAGGCGGGGCGCTGGACAATACACC
P249A	P249A_fw	GTATTGTCCAGCCTCGCGCCTGAAATGG
	P249A_rv	CCATTTTCAGGCGCGAGGCTGGACAATAC
P250A	P250A_fw	TTGTCCAGCCTCCCGGCTGAAATGGATTGTC
	P250A_rv	GACAAATCCATTTTCAGCCGGGAGGCTGG
E251A	E251A_fw	CAGCCTCCCGCCTGCAATGGATTTGTCCC
	E251A_rv	GGGACAAATCCATTGCAGGCGGGAGGCTG
M252A	M252A_fw	CAGCCTCCCGCCTGAAGCGGATTTGTCCAAGTAAAG
	M252A_rv	CTTTACTTGGGACAAATCCGCTTCAGGCGGGAGGCTG

D253A	D253A_fw	CCTCCCGCCTGAAATGGCTTTGTCCCAAGTAAAG
	D253A_rv	CTTTACTTGGGACAAAGCCATTTTCAGGCGGGAGG
L254A	L254A_fw	CTCCCGCCTGAAATGGATGCGTCCCAAGTAAAGTTAC
	L254A_rv	GTAACCTTTACTTGGGACGCATCCATTTTCAGGCGGGAG
S255A	S255A_fw	CGCCTGAAATGGATTTGGCCCAAGTAAAGTTACCG
	S255A_rv	GTAACCTTTACTTGGGCCAAATCCATTTTCAGGCG
Q256A	Q256A_fw	CGCCTGAAATGGATTTGTCCGCAGTAAAGTTACCGTCAAGTG
	Q256A_rv	CACCTTGACGGTAACTTTACTGCGGACAAATCCATTTTCAGGCG
V257A	V257A_fw	GGATTTGTCCCAAGCAAAGTTACCGTCAAGTGG
	V257A_rv	CCACTTGACGGTAACTTTGTCTGGGACAAATCCATTTTC
K258A	K258A_fw	GATTTGTCCCAAGTAGCGTTACCGTCAAGTG
	K258A_rv	CACCTTGACGGTAACTTTACTTGGGACAAATC
L259A	L259A_fw	CCTGAAATGGATTTGTCCCAAGTAAAGGCACCGTCAAGTGGG
	L259A_rv	CCCCTTGACGGTGCCTTTACTTGGGACAAATCCATTTTCAGG
P260A	P260A_fw	GATTTGTCCCAAGTAAAGTTAGCGTCAAGTGGG
	P260A_rv	CCCCTTGACGCTAACTTTACTTGGGACAAATC
S261A	S261A_fw	CAAGTAAAGTTACCGGCAAGTGGGAATCAG
	S261A_rv	CTGATTCCCCTTGCCGGTAACTTTACTTTG
S262A	S262A_fw	CCAAGTAAAGTTACCGTCAAGTGGGAATCAGTTCC
	S262A_rv	GAACTGATTCCCAGCTGACGGTAACTTTACTTGGGAC
G263A	G263A_fw	GTTACCGTCAAGTGCGAATCAGTTCCGGGC
	G263A_rv	GCCCCGAACTGATTTCGCACTTGACGGTAACT
N264A	N264A_fw	GTTACCGTCAAGTGGGGCTCAGTTCCGGGCTAAGTG
	N264A_rv	CACCTTAGCCCCGAACTGAGCCCCACTTGACGGTAACT
F278A	F278A_fw	GACATGGGACCGGCTGGGCCAATGACGATTTTCGCAC
	F278A_rv	GTGCGAAATCGTCATTGGCCCAGCCGGTCCCATGTC
N279A	N279A_fw	CATGGGACCGGCTGGTTTCGCTGACGATTTTCGCACTTC
	N279A_rv	GAAGTGCGAAATCGTCAGCGAACCAGCCGGTCCCATG
D280A	D280A_fw	CTGGTTCAATGCCGATTTTCGCAC
	D280A_rv	GTGCGAAATCGGCATTGAACCAG
D281A	D281A_fw	CGGCTGGTTCAATGACGCTTTTCGCACTTCTGCAAG
	D281A_rv	CTTGCGAAGTGCGAAAGCGTCATTGAACCAGCCG
F282A	F282A_fw	CAATGACGATGCCGCACTTCTGCG
	F282A_rv	GCAGAAGTGCGGCATCGTCATTG
A283G	A283G_fw	GTTCAATGACGATTTTCGGACTTCTGCAAGCCATC
	A283G_rv	GATGGCTTGCAGAAGTCCGAAATCGTCATTGAAC
L284A	L284A_fw	GTTCAATGACGATTTTCGCAAGTGCAGCTTCTGCAAGCCATCATG
	L284A_rv	GATGGCTTGCAGAGCTGCGAAATCGTCATTGAACCAG
L285A	L285A_fw	GACCCATGATGGCTTGCGCAAGTGCGAAATCGTCATTG
	L285A_rv	CAATGACGATTTTCGCACTTGCAGCAAGCCATCATGGGTC
Q286A	Q286A_fw	GACGATTTTCGCACTTCTGGCAGCCATCATGGGTCC
	Q286A_rv	GGACCCATGATGGCTGCCAGAAGTGCGAAATCGTC
A287G	A287G_fw	CGCACTTCTGCAAGCAATCATGGGTCCCTAAGG
	A287G_rv	CCTTAGGACCCATGATTGCTTGCAGAAGTGC
I288A	I288A_fw	CGCACTTCTGCAAGCCGCCATGGGTCCCTAAGGTTG
	I288A_rv	CAACCTTAGGACCCATGGCGGCTTGCAGAAGTGC
M289A	M289A_fw	CACCTTCTGCAAGCCATCGCGGGTCCCTAAGGTTGTGCG
	M289A_rv	CGACAACCTTAGGACCCGCGATGGCTTGCAGAAGTG
G290A	G290A_fw	CTGCAAGCCATCATGGCTCCCTAAGGTTGTGCGATTAC
	G290A_rv	CGACAACCTTAGGAGCCATGATGGCTTGCAG

Supplementary Table 15: Site-directed mutagenesis primers used for saturation of selected loop positions

Mutation	Name	Sequence (5' → 3')
F278NNK	F278NNK_fw	CATGGGACCGGCTGGNNKAATGACGATTTTCGCAC
	F278NNK_rv	GTGCGAAATCGTCATTMNCCAGCCGGTCCCATG
D280NNK	D280NNK_fw	GACCGGCTGGTTCAATNNKGATTTTCGCACTTCTG
	D280NNK_rv	CAGAAGTGCGAAATCMNNATTGAACCAGCCGGTC
D281NNK	D281NNK_fw	CGGCTGGTTCAATGACNNKTTTCGCACTTCTGCAAG
	D281NNK_rv	CTTGCAGAAAGTGCGAAMNNGTCATTGAACCAGCC
F282NNK	F282NNK_fw	CTGGTTCAATGACGATNNKGCACCTTCTGCAAGCC
	F282NNK_rv	GGCTTGCAGAAAGTGCMMNATCGTCATTGAACCAG
A283NNK	A283NNK_fw	GTTCAATGACGATTTTCNNKCTTCTGCAAGCCATC
	A283NNK_rv	GATGGCTTGCAGAAAGMNGAAATCGTCATTGAAC
L284NNK	L284NNK_fw	CAATGACGATTTTCGCANNKCTGCAAGCCATCATGG
	L284NNK_rv	CCATGATGGCTTGCAGMNTGCGAAATCGTCATTG
L285NNK	L285NNK_fw	CAATGACGATTTTCGCACTTNNKCAAGCCATCATGGGTC
	L285NNK_rv	GACCCATGATGGCTTGMNNAAGTGCGAAATCGTCATTG
Q286NNK	Q286NNK_fw	CGATTTTCGCACTTCTGNKGGCCATCATGGGTCCTAAG
	Q286NNK_rv	CTTAGGACCCATGATGGCMNNCAGAAGTGCGAAATCG
A287NNK	A287NNK_fw	GATTTTCGCACTTCTGCAANNKATCATGGGTCCTAAGGTTG
	A287NNK_rv	CAACCTTAGGACCCATGATMNTTGCAGAAAGTGCGAAATC
I288NNK	I288NNK_fw	CGCACTTCTGCAAGCCNNKATGGGTCCTAAGGTTGTC
	I288NNK_rv	GACAACCTTAGGACCCATMNNGGCTTGCAGAAAGTGCG
M289NNK	M289NNK_fw	GCACTTCTGCAAGCCATCNNKGGTCTAAGGTTGTGCG
	M289NNK_rv	CGACAACCTTAGGACCMNNGATGGCTTGCAGAAAGTGC

Supplementary Table 16: Site-directed mutagenesis primers used for the adaption library based on the sequence alignment with oxygenases from *Phenylobacterium immobile* E.

Mutation	Name	Sequence (5' → 3')
T237del	T237del_fw	GTACCATGCGGGAACGGCGCATCTTTTCAGG
	T237del_rv	CCTGAAAGATGCGCCGTTCCCGCATGGTAC
M238del	M238del_fw	GTACCATGCGGGAATGGCGCATCTTTTC
	M238del_rv	GAAAGATGCGCCATTTCCCGCATGGTAC
T237I	T237I_fw	GATATGTACCATGCGGGAATAATGGCGCATC
	T237I_rv	GATGCGCCATTATTTCCCGCATGGTACATATC
A239S	A239S_fw	CATGCGGGAACGATGTCGCATCTTTTCAGGTG
	A239S_rv	CACCTGAAAGATGCGACATCGTTCCCGCATG
L245M	L245M_fw	CATCTTTTCAGGTGTAATGTCCAGCCTCCCGC
	L245M_rv	GCGGGAGGCTGGACATTACACCTGAAAGATG
S247G	S247G_fw	CTTTCAGGTGTATTGTCCGGCCTCCCGCCTGAAATG
	S247G_rv	CATTTTCAGGCGGGAGGCCGACAATACACCTGAAAG
L248F	L248F_fw	GGTGTATTGTCCAGCTTCCCGCCTGAAATGGATTTG
	L248F_rv	CAAATCCATTTTCAGGCGGGAAAGCTGGACAATACACC
P249R	P249R_fw	GTGTATTGTCCAGCCTCCGTCTGAAATGGATTTG
	P249R_rv	CAAATCCATTTTCAGGACGGAGGCTGGACAATACAC
S255L	S255L_fw	CCTGAAATGGATTTGCTGCAAGTAAAGTTACCG
	S255L_rv	CGGTAACCTTACTTGCAGCAAATCCATTTTCAGG
F266H	F266H_fw	GTCAAGTGGGAATCAGCACCGGGCTAAGTGGGGTG
	F266H_rv	CACCCCACTTAGCCCGGTGCTGATTCCCACTTGAC

A268V	A268V_fw	GAATCAGTTCGGGGTAAAGTGGGGTGGACATG
	A268V_rv	CATGTCCACCCCACTTAACCCGGAAGTATTC
W270L	W270L_fw	CAGTTCGGGGCTAAGCTGGGTGGACATGGGACC
	W270L_rv	GGTCCCATGTCCACCCAGCTTAGCCCGGAAGTGG
H273Y	H273Y_fw	GCTAAGTGGGGTGGATATGGGACCGGCTGGTTC
	H273Y_rv	GAACCAGCCGGTCCCATATCCACCCCACTTAGC
T275H	T275H_fw	GTGGGGTGGACATGGGCACGGCTGGTTCAATGAC
	T275H_rv	GTCATTGAACCAGCCGTGCCCATGTCCACCCAC
G276A	G276A_fw	GGTGGACATGGGACCGCCTGGTTCAATGACGATTTTC
	G276A_rv	GAAATCGTCATTGAACCAGCGGTCCCATGTCCACC
W277I	W277I_fw	GGACATGGGACCGGCATTTTCAATGACGATTTTC
	W277I_rv	GAAATCGTCATTGAAAATGCCGGTCCCATGTCC
F278G	F278G_fw	CATGGGACCGGCTGGGGCAATGACGATTTTCGC
	F278G_rv	GCGAAAATCGTCATTGCCCCAGCCGGTCCCATG
D280E	D280E_fw	GACCGGCTGGTTCAATGAAGATTTTCGCACTTCTG
	D280E_rv	CAGAAGTGCGAAATCTTCATTGAACCAGCCGGTC
D281E	D281E_fw	GGCTGGTTCAATGACGAATTCGCACTTCTGCAAG
	D281E_rv	CTTGCAGAAGTGCGAATTCGTCATTGAACCAGCC

Supplementary Table 17: Site-directed insertion mutagenesis primers used for the adaption library based on the sequence alignment with oxygenases from *Phenylobacterium immobile* E.

Mutation	Name	Sequence (5' → 3')
V257_K258 insED	V257InsED_fw	GGATTTGTCCCAAGTAGAAGACAAGTTACCGTCAAGTGG
	V257InsED_rv	CCACTTGACGGTAACTTGTCTTCTACTTGGGACAAATCC
V257_K258 insEDQE	V257InsEDQE_fw	GGATTTGTCCCAAGTAGAAGACCAGGAAAAGTTACCGTCAA GTGG
	V257InsEDQE_rv	CCACTTGACGGTAACTTTTCTTCTACTTGGGACAA ATCC
V257_K258 insEDQEL A	V257InsEDQELA_fw	GGATTTGTCCCAAGTAGAAGACCAGGAACTGGCGAAGTTAC CGTCAAGTGG
	V257InsEDQELA_rv	CCACTTGACGGTAACTTCGCCAGTTCCTGGTCTTCTACTTG GGACAAATCC
V257_K258 insEDQEL ARI	V257InsEDQELARI_fw	GGATTTGTCCCAAGTAGAAGACCAGGAACTGGCGCGTATTA AGTTACCGTCAAGTGG
	V257InsEDQELARI_rv	CCACTTGACGGTAACTTAATACGCGCCAGTTCCTGGTCTTC TACTTGGGACAAATCC
V257_K258 insEDQEL ARIA	V257InsEDQELARIA_fw	GGATTTGTCCCAAGTAGAAGACCAGGAACTGGCGCGTATTG CGAAGTTACCGTCAAGTGG
	V257InsEDQELARIA_rv	CCACTTGACGGTAACTTCGCAATACGCGCCAGTTCCTGGTC TTCTACTTGGGACAAATCC
L259_P260 insG	L259InsG_fw	GATTTGTCCCAAGTAAAGTTAGGCCCGTCAAGTGGGAATC
	L259InsG_rv	GATTCCCCTTGACGGGCTAACTTTACTTGGGACAAATC
P260_S261 insG	L260InsG_fw	GTCCCAAGTAAAGTTACCGGGCTCAAGTGGGAATCAG
	L260InsG_rv	CTGATTCCCCTTGACGGGCTAACTTTACTTGGGAC
V257_K258 insEE	V257InsEE_fw	GGATTTGTCCCAAGTAGAAGAAAAGTTACCGTCAAGTGG
	V257InsEE_rv	CCACTTGACGGTAACTTTTCTTCTACTTGGGACAAATCC
V257_K258 insEERE	V257InsEERE_fw	GGATTTGTCCCAAGTAGAAGAACGCGAAAAGTTACCGTCAA GTGG
	V257InsEERE_rv	CCACTTGACGGTAACTTTTCTTCTACTTGGGACAA ATCC

V257_K258 insEEREL A	V257InsEERELA_fw	GGATTTGTCCCAAGTAGAAGAACGCGAACTGGCAAAGTTAC CGTCAAGTGG
	V257InsEERELA_rv	CCACTTGACGGTAACTTTGCCAGTTCGCGTTCTTCTACTTG GGACAAATCC
V257_K258 insEEREL AA	V257InsEERELAA_fw	GGATTTGTCCCAAGTAGAAGAACGCGAACTGGCGGCAAAGT TACCGTCAAGTGG
	V257InsEERELAA_rv	CCACTTGACGGTAACTTTGCCGCCAGTTCGCGTTCTTCTAC TTGGGACAAATCC
K258_L259 insAG	K258InsAG_fw	GATTTGTCCCAAGTAAAGGCGGGCTTACCGTCAAGTGGG
	K258InsAG_rv	CCCACTTGACGGTAAAGCCCGCTTTACTTGGGACAAATC
L259_P260 insA	L259InsA_fw	GATTTGTCCCAAGTAAAGTTAGCGCCGTCAAGTGGGAATC
	L259InsA_rv	GATTTCCACTTGACGGCGCTAACTTTACTTGGGACAAATC
P260_S261 insGS	P260InsGS_fw	GTCCCAAGTAAAGTTACCGGGTAGCTCAAGTGGGAATCAG
	P260InsGS_rv	CTGATTTCCACTTGAGCTACCCGGTAACTTTACTTGGGAC
P260_S261 insGG	P260InsGG_fw	GTCCCAAGTAAAGTTACCGGGTGGTTC AAGTGGGAATCAG
	P260InsGG_rv	CTGATTTCCACTTGAACCACCCGGTAACTTTACTTGGGAC
N279_D280 insE	N279InsE_fw	GGGACCGGCTGGTTCAATAACGACGATTTTCGCACTTC
	N279InsE_rv	GAAGTGCGAAAATCGTCGTTATTGAACCAGCCGGTCCC
Q286_A287 insKK	Q286InsKK_fw	CGATTTTCGCACTTCTGCAAAAAAAGCCATCATGGGTCCTA AG
	Q286InsKK_rv	CTTAGGACCCATGATGGCTTTTTTTTTGCAGAAGTGC GAAAT CG
Q286_A287 insKKAA	Q286InsKKAA_fw	CGATTTTCGCACTTCTGCAAAAAAAGCGGCGGCCATCATGG GTCCTAAG
	Q286InsKKAA_rv	CTTAGGACCCATGATGGCCGCGCTTTTTTTTTGCAGAAGTG CGAAATCG
Q286_A287 insKKAAE G	Q286InsKKAAEG_fw	CGATTTTCGCACTTCTGCAAAAAAAGCGGCGGAAGGCGCCA TCATGGGTCCCTAAG
	Q286InsKKAAEG_rv	CTTAGGACCCATGATGGCGCCTTCCGCGCTTTTTTTTTGCA GAAGTGCGAAAATCG
F278_N279 insGP	F278InsGP_fw	CATGGGACCGGCTGGTTCGGCCAAATGACGATTTTCGCAC
	F278InsGP_rv	GTGCGAAATCGTCATTTGGGCCGAACCAGCCGGTCCCATG
F278_N279 insGPRL	F278InsGPRL_fw	CATGGGACCGGCTGGTTCGGCCACGTCTGAATGACGATTT CGCAC
	F278InsGPRL_rv	GTGCGAAATCGTCATTCAGACGTGGGCCGAACCAGCCGGTC CCATG
Q286_A287 insEM	N279InsP_fw	GGGACCGGCTGGTTC AATCCGACGATTTTCGCACTTC
	N279InsP_rv	GAAGTGCGAAAATCGTCCGATTGAACCAGCCGGTCCC
Q286_A287 insEM	Q286InsEM_fw	CGATTTTCGCACTTCTGCAAGAAATGGCCATCATGGGTCCTA AG
	Q286InsEM_rv	CTTAGGACCCATGATGGCCATTTCTTGCAGAAGTGC GAAAT CG
Q286_A287 insEMKA	Q286InsEMKA_fw	CGATTTTCGCACTTCTGCAAGAAATGAAAGCCGCCATCATGG GTCCTAAG
	Q286InsEMKA_rv	CTTAGGACCCATGATGGCGGCTTTCATTTCTTGCAGAAGTG CGAAATCG
Q286_A287 insEMKAE G	Q286InsEMKAEG_fw	CGATTTTCGCACTTCTGCAAGAAATGAAAGCCGAAGGCGCCA TCATGGGTCCCTAAG
	Q286InsEMKAEG_rv	CTTAGGACCCATGATGGCGCCTTCCGCTTTCATTTCTTGC GAAGTGCGAAAATCG
Q286_A287	Q286InsEMKAEGK_fw	CGATTTTCGCACTTCTGCAAGAAATGAAAGCCGAAGGCAAAG CCATCATGGGTCCCTAAG

insEMKAE	Q286InsEMKAEGK_rv	CTTAGGACCCATGATGGCTTTGCCTTCGGCTTTCATTTCTT
GK		GCAGAAGTGCGAAATCG

Supplementary Table 18: Site-directed mutagenesis primers used for the deletion variants. * = mutations incorporated by overlap PCR

Mutation	Name	Sequence (5' → 3')
E251del	P250DelE_fw	GTCCAGCCTCCCGCCTATGGATTTGTCCCAAGTAAAGTTACCG
	P250DelE_rv	AGGCGGGAGGCTGGACAATACACCTGAAAGATGCGCCATC
	P249DelPEM_	CAGGTGTATTGTCCAGCCTCCCGGATTTGTCCCAAGTAAAGTTACC
P250_M252 del	fw	
	P249DelPEM_rv	GGTAACTTTACTTGGGACAAATCCGGGAGGCTGGACAATACACCTG
L248_L254 del *	S247DelLPPE	CGCATCTTTCAGGTGTATTGTCCAGCTCCCAAGTAAAGTTACCGTCA
	MDL_fw	AGTGGG
	S247DelLPPE	GCTGGACAATACACCTGAAAGATGCGCCATCGTTCCCGCATGGTACA
V257del	MDL_rv	TATC
	Q256DelV_fw	GCCTGAAATGGATTTGTCCAAAAGTTACCGTCAAGTGGGAATCAGT
	TC	
Q256_K258 del	Q256DelV_rv	TTGGGACAAATCCATTTTCAGGCGGGAGGCTGGACAATACACCTG
	S255DelQVK_	CGCCTGAAATGGATTTGTCTTACCGTCAAGTGGGAATCAGTTCCG
	fw	
L254_P260 del *	S255DelQVK_rv	GGACAAATCCATTTTCAGGCGGGAGGCTGGACAATACACCTGAAAG
	D253DelLSQ	GCCTCCCGCCTGAAATGGATTCAAGTGGGAATCAGTTCCGGGCTAAG
	VKLP_fw	
A283del	D253DelLSQ	ATCCATTTTCAGGCGGGAGGCTGGACAATACACCTGAAAGATGCGCC
	VKLP_rv	
	F282DelA_fw	GGCTGGTTCAATGACGATTTCTTCTGCAAGCCATCATGGGTTC
F282_L284 del	F282DelA_rv	GAAATCGTCATTGAACCAGCCGGTCCCATGTCCACCCAC
	D281DelFAL_	CCGGCTGGTTCAATGACGATCTGCAAGCCATCATGGGTTC
	fw	
D280_Q286 del *	D281DelFAL_rv	TCGTTCATTGAACCAGCCGGTCCCATGTCCACCCCACTTAGC
	N279DelIDDF	CATGGGACCGGCTGGTTCAATGCCATCATGGGTCCCTAAGTTGTCTG
	ALLQ_fw	
	N279DelIDDF	ATTGAACCAGCCGGTCCCATGTCCACCCCACTTAGCCCGG
	ALLQ_rv	

Supplementary Table 19: Site-directed mutagenesis primers used for the LILI library after position V257.

Mutation	Name	Sequence (5' → 3')
V257_K258 insGG	V257_K258ins GG_fw	GGATTTGTCCCAAGTAGGTGGTAAGTTACCGTCAAGTGG
	V257_K258ins GG_rv	CCACTTGACGGTAACTTACCACCTACTTGGGACAAATCC
V257_K258 insGGG	V257_K258ins GGG_fw	GGATTTGTCCCAAGTAGGTGGTGGTAAGTTACCGTCAAGTGG
	V257_K258ins GGG_rv	CCACTTGACGGTAACTTACCACCACCTACTTGGGACAAATCC
V257_K258 insGGGG	V257_K258ins GGGG_fw	GGATTTGTCCCAAGTAGGTGGTGGTGGTAAGTTACCGTCAAGTGG
	V257_K258ins GGGG_rv	CCACTTGACGGTAACTTACCACCACCACCTACTTGGGACAAATCC
V257_K258 insGGGGG	V257_K258ins GGGGG_fw	GGATTTGTCCCAAGTAGGTGGTGGTGGTGGTAAGTTACCGTCAAGTG G
	V257_K258ins GGGGG_rv	CCACTTGACGGTAACTTACCACCACCACCACCTACTTGGGACAAATC C
V257_K258 insGGGGG G	V257_K258ins GGGGGG_fw	GGATTTGTCCCAAGTAGGTGGTGGTGGTGGTGGTAAGTTACCGTCAA GTGG
	V257_K258ins GGGGGG_rv	CCACTTGACGGTAACTTACCACCACCACCACCACCTACTTGGGACAA ATCC
V257_K258 insGS	V257_K258ins GS_fw	GGATTTGTCCCAAGTAGGTTCTAAGTTACCGTCAAGTGG
	V257_K258ins GS_rv	CCACTTGACGGTAACTTAGAACCTACTTGGGACAAATCC
V257_K258 insGSG	V257_K258ins GSG_fw	GGATTTGTCCCAAGTAGGTTCTGGTAAGTTACCGTCAAGTGG
	V257_K258ins GSG_rv	CCACTTGACGGTAACTTAGAACCCAGATACTTGGGACAAATCC
V257_K258 insGSGS	V257_K258ins GSGS_fw	GGATTTGTCCCAAGTAGGTTCTGGTCTAAGTTACCGTCAAGTGG
	V257_K258ins GSGS_rv	CCACTTGACGGTAACTTAGAACCCAGAACCCTACTTGGGACAAATCC
V257_K258 insGSGSG	V257_K258ins GSGSG_fw	GGATTTGTCCCAAGTAGGTTCTGGTCTGGTAAGTTACCGTCAAGTG G
	V257_K258ins GSGSG_rv	CCACTTGACGGTAACTTAGAACCCAGAACCAGATACTTGGGACAAATC C
V257_K258 insGSGSG S	V257_K258ins GSGSGS_fw	GGATTTGTCCCAAGTAGGTTCTGGTCTGGTCTAAGTTACCGTCAA GTGG
	V257_K258ins GSGSGS_rv	CCACTTGACGGTAACTTAGAACCCAGAACCAGAACCCTACTTGGGACAA ATCC
V257_K258 insPA	V257_K258ins PA_fw	GGATTTGTCCCAAGTACCGGCAAAGTTACCGTCAAGTGG
	V257_K258ins PA_rv	CCACTTGACGGTAACTTTGCCGGTACTTGGGACAAATCC
V257_K258 insPAP	V257_K258ins PAP_fw	GGATTTGTCCCAAGTACCGGCACCGAAGTTACCGTCAAGTGG
	V257_K258ins PAP_rv	CCACTTGACGGTAACTTCGGTGCCGGTACTTGGGACAAATCC

V257_K258 insPAPA	V257_K258ins	GGATTTGTCCCAAGTACCGGCACCGGCACCGCAAAGTTACCGTCAAGTGG
	PAPA_fw V257_K258ins PAPA_rv	CCACTTGACGGTAACTTTGCCGGTGCCGGTACTTGGGACAAATCC
V257_K258 insPAPAP	V257_K258ins	GGATTTGTCCCAAGTACCGGCACCGGCACCGAAGTTACCGTCAAGTG
	PAPAP_fw V257_K258ins PAPAP_rv	G CCACTTGACGGTAACTTCGGTGCCGGTGCCGGTACTTGGGACAAATC C
V257_K258 insPAPAP A	V257_K258ins	GGATTTGTCCCAAGTACCGGCACCGGCACCGCAAAGTTACCGTCAA
	PAPAPA_fw V257_K258ins PAPAPA_rv	GTGG CCACTTGACGGTAACTTTGCCGGTGCCGGTGCCGGTACTTGGGACAA ATCC
V257_K258 insGP	V257_K258ins	GGATTTGTCCCAAGTAGGTCCGAAGTTACCGTCAAGTGG
	GP_fw V257_K258ins GP_rv	CCACTTGACGGTAACTTCGGACCTACTTGGGACAAATCC
V257_K258 insGPG	V257_K258ins	GGATTTGTCCCAAGTAGGTCCGGGTAAAGTTACCGTCAAGTGG
	GPG_fw V257_K258ins GPG_rv	CCACTTGACGGTAACTTACCCGGACCTACTTGGGACAAATCC
V257_K258 insGPGP	V257_K258ins	GGATTTGTCCCAAGTAGGTCCGGGTCCGAAGTTACCGTCAAGTGG
	GPGP_fw V257_K258ins GPGP_rv	CCACTTGACGGTAACTTCGGACCCGGACCTACTTGGGACAAATCC
V257_K258 insGPGPG	V257_K258ins	GGATTTGTCCCAAGTAGGTCCGGGTCCGGGTAAAGTTACCGTCAAGTG
	GPGPG_fw V257_K258ins GPGPG_rv	G CCACTTGACGGTAACTTACCCGGACCCGGACCTACTTGGGACAAATC C
V257_K258 insGPGPG P	V257_K258ins	GGATTTGTCCCAAGTAGGTCCGGGTCCGGGTCCGAAGTTACCGTCAA
	GPGPGP_fw V257_K258ins GPGPGP_rv	GTGG CCACTTGACGGTAACTTCGGACCCGGACCCGGACCTACTTGGGACAA ATCC

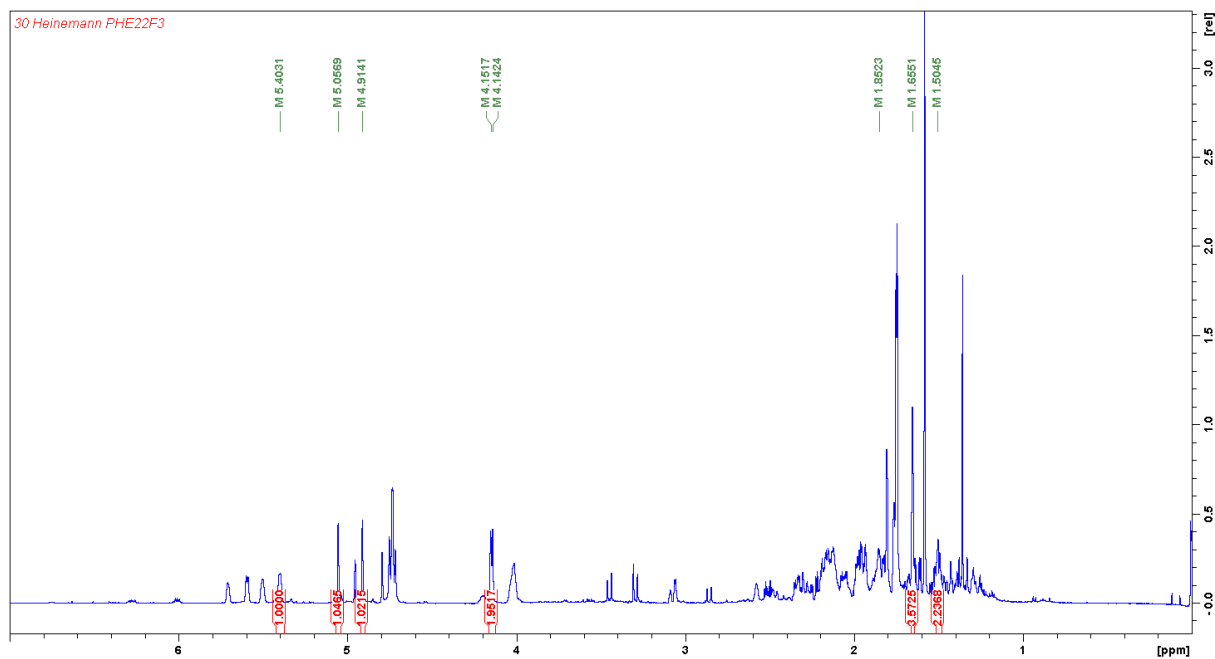
F278_N279 insPAPA	F278_N279ins	GGACATGGGACCGGCTGGTTC	CCCGGCACCGGCAAATGACGATTTTCGC
	PAPA_fw	ACTTC	
	F278_N279ins	GAAGTGC	GAAATCGTCATTTGCCGGTGCCGGGAACCAGCCGGTCCCA
	PAPA_rv	TGTCC	
F278_N279 insPAPAP	F278_N279ins	GGACATGGGACCGGCTGGTTC	CCCGGCACCGGCAATGACGATTT
	PAPAP_fw	CGCACTTC	
	F278_N279ins	GAAGTGC	GAAATCGTCATTCGGTGCCGGTGCCGGGAACCAGCCGGTC
	PAPAP_rv	CCATGTCC	
F278_N279 insPAPAP A	F278_N279ins	GGACATGGGACCGGCTGGTTC	CCCGGCACCGGCAAATGACGA
	PAPAPA_fw	TTTCGCACTTC	
	F278_N279ins	GAAGTGC	GAAATCGTCATTTGCCGGTGCCGGTGCCGGGAACCAGCCG
	PAPAPA_rv	GTCCCATGTCC	
F278_N279 insGP	F278_N279ins	GGACATGGGACCGGCTGGTTC	CGGTCCGAATGACGATTTTCGCACTTC
	GP_fw		
	F278_N279ins	GAAGTGC	GAAATCGTCATTCGGACCGAACCAGCCGGTCCCATGTCC
	GP_rv		
F278_N279 insGPG	F278_N279ins	GGACATGGGACCGGCTGGTTC	CGGTCCGGGTAATGACGATTTTCGCACT
	GPG_fw	TC	
	F278_N279ins	GAAGTGC	GAAATCGTCATTACCCGGACCGAACCAGCCGGTCCCATGT
	GPG_rv	CC	
F278_N279 insGPGP	F278_N279ins	GGACATGGGACCGGCTGGTTC	CGGTCCGGGTCCGAATGACGATTTTCGC
	GPGP_fw	ACTTC	
	F278_N279ins	GAAGTGC	GAAATCGTCATTCGGACCCGGACCGAACCAGCCGGTCCCA
	GPGP_rv	TGTCC	
F278_N279 insGPGPG	F278_N279ins	GGACATGGGACCGGCTGGTTC	CGGTCCGGGTCCGGGTAATGACGATTT
	GPGPG_fw	CGCACTTC	
	F278_N279ins	GAAGTGC	GAAATCGTCATTACCCGGACCCGGACCGAACCAGCCGGTC
	GPGPG_rv	CCATGTCC	
F278_N279 insGPGPG P	F278_N279ins	GGACATGGGACCGGCTGGTTC	CGGTCCGGGTCCGGGTCCGAATGACGA
	GPGPGP_fw	TTTCGCACTTC	
	F278_N279ins	GAAGTGC	GAAATCGTCATTCGGACCCGGACCCGGACCGAACCAGCCG
	GPGPGP_rv	GTCCCATGTCC	

Supplementary Table 21: Site-directed mutagenesis primers used for the LILI library after position Q286.

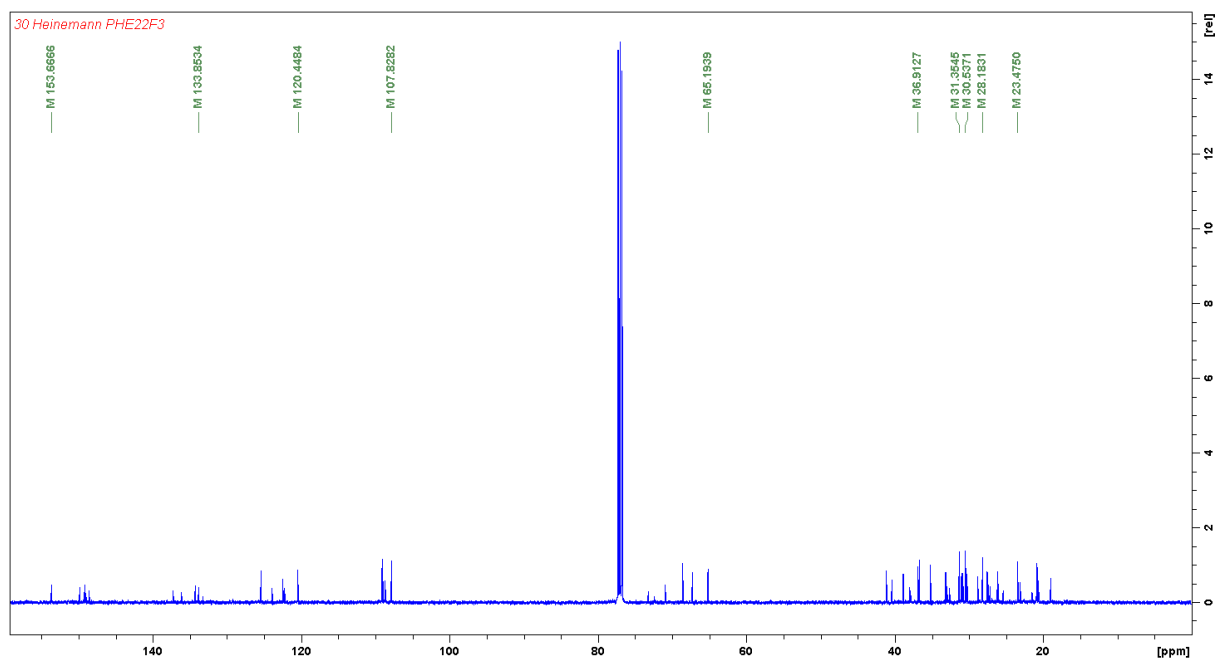
Mutation	Name	Sequence (5' → 3')
Q286_A287 insGG	Q286_A287ins GG_fw	GACGATTTTCGCACTTCTGCAAGGTGGTGCCATCATGGGTCCTAAGG
	Q286_A287ins GG_rv	CCTTAGGACCCATGATGGCACCACCTTGCAGAAGTGCGAAATCGTC
Q286_A287 insGGG	Q286_A287ins GGG_fw	GACGATTTTCGCACTTCTGCAAGGTGGTGCCATCATGGGTCCTAA GG
	Q286_A287ins GGG_rv	CCTTAGGACCCATGATGGCACCACCACCTTGCAGAAGTGCGAAATCG TC
Q286_A287 insGGGG	Q286_A287ins GGGG_fw	GACGATTTTCGCACTTCTGCAAGGTGGTGCCATCATGGGTC TAAGG
	Q286_A287ins GGGG_rv	CCTTAGGACCCATGATGGCACCACCACCACCTTGCAGAAGTGCGAAA TCGTC
Q286_A287 insGGGGG	Q286_A287ins GGGGG_fw	GACGATTTTCGCACTTCTGCAAGGTGGTGCCATCATGGG TCCTAAGG
	Q286_A287ins GGGGG_rv	CCTTAGGACCCATGATGGCACCACCACCACCACCTTGCAGAAGTGCG AAATCGTC
Q286_A287 insGGGGG G	Q286_A287ins GGGGGG_fw	GACGATTTTCGCACTTCTGCAAGGTGGTGCCATCATGGG GGGTCCTAAGG
	Q286_A287ins GGGGGG_rv	CCTTAGGACCCATGATGGCACCACCACCACCACCACCTTGCAGAAGT GCGAAATCGTC
Q286_A287 insGS	Q286_A287ins GS_fw	GACGATTTTCGCACTTCTGCAAGGTTCTGCCATCATGGGTCCTAAGG
	Q286_A287ins GS_rv	CCTTAGGACCCATGATGGCAGAACCTTGCAGAAGTGCGAAATCGTC
Q286_A287 insGSG	Q286_A287ins GSG_fw	GACGATTTTCGCACTTCTGCAAGGTTCTGGTGCCATCATGGGTCCTAA GG
	Q286_A287ins GSG_rv	CCTTAGGACCCATGATGGCACCAGAACCTTGCAGAAGTGCGAAATCG TC
Q286_A287 insGSGS	Q286_A287ins GSGS_fw	GACGATTTTCGCACTTCTGCAAGGTTCTGGTTCTGCCATCATGGGTC TAAGG
	Q286_A287ins GSGS_rv	CCTTAGGACCCATGATGGCAGAACCAGAACCTTGCAGAAGTGCGAAA TCGTC
Q286_A287 insGSGSG	Q286_A287ins GSGSG_fw	GACGATTTTCGCACTTCTGCAAGGTTCTGGTTCTGGTGCCATCATGGG TCCTAAGG
	Q286_A287ins GSGSG_rv	CCTTAGGACCCATGATGGCACCAGAACCAGAACCTTGCAGAAGTGCG AAATCGTC
Q286_A287 insGSGSG S	Q286_A287ins GSGSGS_fw	GACGATTTTCGCACTTCTGCAAGGTTCTGGTTCTGGTTCTGCCATCAT GGGTCCTAAGG
	Q286_A287ins GSGSGS_rv	CCTTAGGACCCATGATGGCAGAACCAGAACCAGAACCTTGCAGAAGT GCGAAATCGTC
Q286_A287 insPA	Q286_A287ins PA_fw	GACGATTTTCGCACTTCTGCAACCAGCCATCATGGGTCCTAAGG
	Q286_A287ins PA_rv	CCTTAGGACCCATGATGGCTGCCGGTTGCAGAAGTGCGAAATCGTC
Q286_A287 insPAP	Q286_A287ins PAP_fw	GACGATTTTCGCACTTCTGCAACCAGCCATCATGGGTCCTAA GG
	Q286_A287ins PAP_rv	CCTTAGGACCCATGATGGCCGGTGCCGGTTGCAGAAGTGCGAAATCG TC

Q286_A287 insPAPA	Q286_A287ins	GACGATTTTCGCACTTCTGCAACCGGCACCGGCAGCCATCATGGGTCC
	PAPA_fw	TAAGG
	Q286_A287ins	CCTTAGGACCCATGATGGCTGCCGGTGCCGGTTGCAGAAGTGCGAAA
	PAPA_rv	TCGTC
Q286_A287 insPAPAP	Q286_A287ins	GACGATTTTCGCACTTCTGCAACCGGCACCGGCACCGGCCATCATGGG
	PAPAP_fw	TCCTAAGG
	Q286_A287ins	CCTTAGGACCCATGATGGCCGGTGCCGGTGCCGGTTGCAGAAGTGC
	PAPAP_rv	AAATCGTC
Q286_A287 insPAPAP A	Q286_A287ins	GACGATTTTCGCACTTCTGCAACCGGCACCGGCACCGGCAGCCATCAT
	PAPAPA_fw	GGGTCCTAAGG
	Q286_A287ins	CCTTAGGACCCATGATGGCTGCCGGTGCCGGTGCCGGTTGCAGAAGT
	PAPAPA_rv	GCGAAATCGTC
Q286_A287 insGP	Q286_A287ins	GACGATTTTCGCACTTCTGCAAGGTCCGGCCATCATGGGTCCCTAAGG
	GP_fw	
	Q286_A287ins	CCTTAGGACCCATGATGGCCGGACCTTGCAGAAGTGCGAAATCGTC
	GP_rv	
Q286_A287 insGPG	Q286_A287ins	GACGATTTTCGCACTTCTGCAAGGTCCGGGTGCCATCATGGGTCCCTAA
	GPG_fw	GG
	Q286_A287ins	CCTTAGGACCCATGATGGCACCCGGACCTTGCAGAAGTGCGAAATCG
	GPG_rv	TC
Q286_A287 insGPGP	Q286_A287ins	GACGATTTTCGCACTTCTGCAAGGTCCGGGTCCGGCCATCATGGGTCC
	GPGP_fw	TAAGG
	Q286_A287ins	CCTTAGGACCCATGATGGCCGGACCCGGACCTTGCAGAAGTGCGAAA
	GPGP_rv	TCGTC
Q286_A287 insGPGPG	Q286_A287ins	GACGATTTTCGCACTTCTGCAAGGTCCGGGTCCGGGTGCCATCATGGG
	GPGPG_fw	TCCTAAGG
	Q286_A287ins	CCTTAGGACCCATGATGGCACCCGGACCCGGACCTTGCAGAAGTGC
	GPGPG_rv	AAATCGTC
Q286_A287 insGPGPG P	Q286_A287ins	GACGATTTTCGCACTTCTGCAAGGTCCGGGTCCGGGTCCGGCCATCAT
	GPGPGP_fw	GGGTCCTAAGG
	Q286_A287ins	CCTTAGGACCCATGATGGCCGGACCCGGACCCGGACCTTGCAGAAGT
	GPGPGP_rv	GCGAAATCGTC

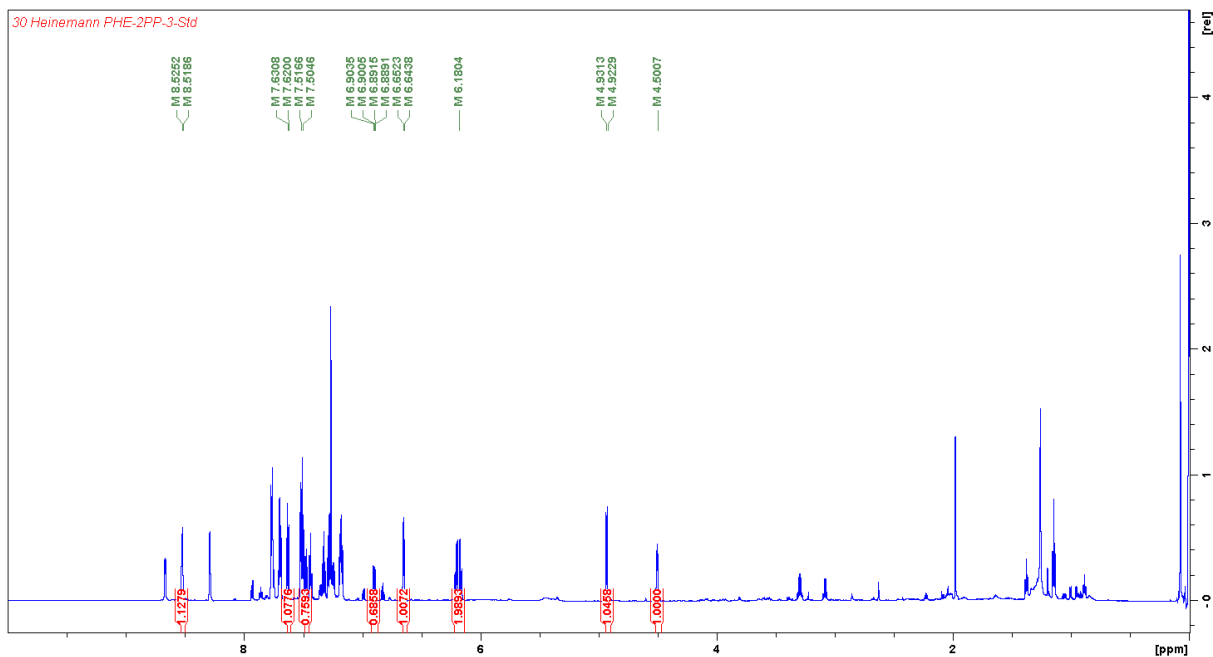
NMR spectra



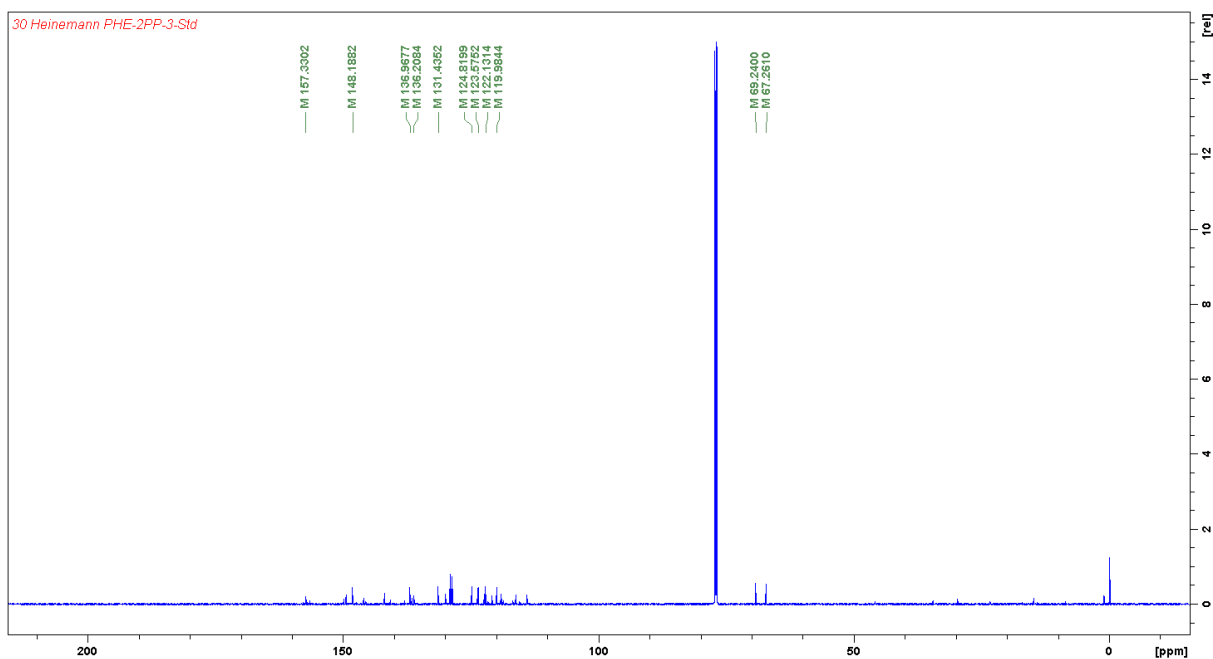
Supplementary Fig. 29: ^1H -NMR of the product of the synthesis of (+)-mentha-1.8-dien-10-ol **2b** in CDCl_3



Supplementary Fig. 30: ^{13}C -NMR of the product of the synthesis of (+)-mentha-1.8-dien-10-ol **2b** in CDCl_3



Supplementary Fig. 31: ^1H -NMR of the in-house standard of 1,2-dihydroxy-3-(2'-pyridyl)-cyclohexa-3,5-diene 3a.



Supplementary Fig. 32: ^{13}C -NMR of the in-house standard of 1,2-dihydroxy-3-(2'-pyridyl)-cyclohexa-3,5-diene 3a.

Sequence of the Cumene Dioxygenase from *Pseudomonas fluorescens* IP01

CDO gene cluster (GenBank: D37828.1)¹¹

cumA1 (Oxygenase α -subunit) → **cumA2** (Oxygenase β -subunit) → **cumA3** (Ferredoxin) → **cumA4** (Reductase)

Overlapping sequence space between cumA3 and cumA4 is underlined.

```
ATGAGTTCAATAATAAATAAAGAAGTGCAGGAAGCCCTTTGAAATGGGTGAAAACTGGTCTGACGAGGAGATTAAGCGCT
CGTTGATGAGGAAAAGGGGTGCTTGATCCACGATTTTTCTCTGATCAGGATTTGTATGAGATCGAGCTTGAGAGGGTGTG
CTCGATCCTGGCTGCTTGGGCACGAGGGGCACATTCCAAAGCCGGGATTATCTGACCACCTACATGGGTGAAGACCCA
GTAATTGTAGTGAGGCAGAAAGACCGGAGCATTAAAGTCTTTTTAAACCAATGTCGGCATCGCGGTATGCGTATTGAGCGATC
GGATTTGGCAACGCAAAGTCATTTACCTGCACTTATCACGGGTGGGCTATGACACCGCCGTAATCTGGTCAATGTACCCCT
ACGAGAAAGAGGCTTTTTGTGACAAAAAGAGGGTACTGCGGGTTCGACAAGGCCGACTGGGGGCCGTGCAAGCGCGGGTG
GATACTTACAAGGGCTGATTTTTGCCAACCTGGGATACCGAAGCCCTGATTTGAAGACCTATCTGAGCGATGCAACACCTA
TATGGACGTGATGCTCGATCGGACCGAGGCAGTTACTCAGGTCAACCCGGTATGCAAAAACGCGTAATCCCTGTAACCTGGA
AATTCGCGCCGAGCAATCTGTAGCGATATGTACCATGCGGGAACGATGGCGCATCTTTCAGGTGTATTGTCCAGCCTCCCG
CCTGAAATGGATTTGTCCTCAAGTAAAGTTACCGTCAAGTGGGAATCAGTTCCGGGCTAAGTGGGGTGGACATGGGACCGCTG
GTTCAATGACGATTTGCGCACTTCTGCAAGCCATCATGGGTCTAAGGTTGTGCGATTACTGGACCAAAGGTCACAGCTGCTGAGC
GTGCAAAAAGAGCGTCTGGGTAAGTCTTCCGGCTGATCGCATGGTTGCTCAGCATATGACCATTTTTCCGACATGCTCATT
CTTCTGGCATCAATACAGTCCGTAATTTGGCACCACGTTGGCCCTAATGAGATCGAAGTTTGGTCTTTCATCGTAGTGGATGC
TGATGCACCTGAAGATATCAAGGAAGAATATCGTCCGAAAAACATCTTCACCTCAATCAAGGGGGAACCTACGAGCAGGACG
ATGGCGAAAACCTGGGTGGAGGTTACGCGGGGATTCGCGGGCTACAAGGCTAGAAGTAGACCTCTTTGTGCCAGATGGGGCGG
GGTGTGCCAAACAAGAAACAACCCGGAGTTTCTGGAAAAGACCAGTACGTTTATAGCGAAGAAGCTCGCGGAGGGTCTACCA
CCACTGGAGCCGCATGATGTCGAGCCGAGTTGGGACACGCTAAAGTCTTGAGCAGATAAAGTGACCGAAAAAAGCAATCACT
TTCATCGGGTTTCTACCGTGGTAGACAAGGGTTTAGCCTGTTTTTGGTTGCTGGAAGTGCCTAAGTGAATTGATTAACCTGG
GTAAACCCCTGGCTTTGTGCGGGGTATTTACTCGGGTGCATTCCAAATGTACAGCTGTGCGTTTGGTGATAATCGTCATGCT
ATGGATTTGCTATTTGCATGAGCCGAGTGCAGGTGCGCCAACATATATACAGGAACTAATTATGACATCCGCTGATTTGACA
AAACCCATCGAGTGGCCAGAAATGCCCGTCAGTCTTGAATTGCAAAATGCCGTTGAGCAATTTACTATCGCGAAGCACAGTT
GCTTGATATCAAACATGATGAGGCTGGCTGGCTTTACTGACCAAGACATCCAATATGGATGCCAATTCGTACTCTACTCATA
ATCCCGGAATAAGCGATGAGTACGTTGCCCCCGGTAAGTCCCATTTTACGAGACGATGAGAGCAGTATGAGTCTGCGCGC
ATTCGGGCGAGGTTTTCGGGGCTTAACTGGACTGAAGTCCACCGTCCGCGCAGCCGGCACATTGTAAGCAACGTTATCGTCCG
CGAACTGAGAGTCTGGTACTTTGGAAGTAGTTCTGCGTTCCTTTGTACCCTAATCGATTGGAGCGTATGACGGACATCT
ATGTCGGTGAGCGTCGAGATATTTGCTCCGTGTAAGTACGCGGGTGGGATTCAAAATGCCAAGCGAACGATCTTGCTCGAC
CAGAGCACGATTACAGCGAATAATCTCAGCCAGTTTTTCTAACTAGGGAATGCTGGCCACTTACCCTATACCCAGCCTATTC
TGAGAGCGGCCTGAAAATGAAGAGGAGCTACCCGATAGCTACGCAAACTAATCGCGCTCGCCCTTCTCTGATCGCGATCGGTA
CTTTTACTTGGCCAACTCTCCTCGGACTTTGCATTTACAGCAGCTGCGGCTGTTCGGCATGATGTATTCGGGTGTGGATTTG
CAGGTCGGCGCTCCGGTATTACCCCTGCTGCAGGATGCTTGGGCCGTAGTTCGGGCTGACGCTGGGGGGCACTGGGCTGGTTG
GTTGTGGGGCGCACGTCAGCCCGTGCCTTCATGGCGGTTGTCCCGTGGTTCATCGTCACGGAAGTGTGCGACGGTATCTGGG
ACTTGTACAGCATCGTTTGGAGTACGAAAGCCATGTGGTTCGGGCTCCTGACGTTCCGCATCCACGTTGGTGTGGATCGTCTGG
GGTTACAGGTATGGCGCGTGTGCTCTGCGCGGTATCTGGCTTAAACGTCCTCAACCTCCTGAATCTGTGGCCTGAATTGAA
CTCTGTCAATTTCCCATGCGCGTGCAGCTTATCCGGCGCTTGCGCCAAGCTGGCTGCCGATTTAATGAGTAGTTAAAGTTAG
CTATAGAAACTCTGAAAAAGGCTTACCTCATGAGATATCCAGTCTGCAGTCCGCGTGGTTACTGGCGTGCATTTTCCGAGTG
CGTACTTTTTAGACCAACTCTATAATAAGAGACAAAAAGAATGACTTTTTTCAAAGTTTGTGAAGTATCTGATGTGCCCGT
CGGTGACGCTTGCAGGTTGAAAGTAAAGGCGAAGCCGTCGCGATTTTCAACGTCGATGGAGAGTTGTTTCGCAACACAGGACC
GTTGCACTCATGGTACTGGTCTTGTCCGAAGCGGCTACCTAGAGGGTGACATTTGTCGAATGCTCGTGCACATGGGTAGG
TTCTGTGTCCGCACGGCAAGGTAAGGACAGCACCCGCTGTGAGCCGCTGAAGATATATCCGATTCGAATAGATGGCAGCGA
TGTGTTTCGTAGACTTTGATGCCGGGTATCTAGCGCCATGATTAATCAATCGTCATTATTTGGTGCTGGCTTGGCTGGCGAAC
TGCCACTCGCTATCTTCGCGCCCAAGGATATCAGGGAAAGATCCATCTGGTTCGGGGAGGAGTTGCATGTGGCTTACGATCGCC
CCTCCTTATCCAAGGACACCCGTGTCAGGAAAAGTGGTTCGAACCACCCGCAATCCTGGATCCTTGTGGTATGCATCGGCCGAT
ATAGATCTCCATTTAGGTGTACCGGTGACCGGTATTGATGTGTGTAACCACCCAGGTACTTTTCAATCCGGTGACATTTCTAGC
CTACGACCGACTGCTATTAGCCACCGCGCTCGCGCGCGGCTATGGCTATTACGGGAAGCGAGTTGGCCGGCATTACACCT
TGCGTGACCGCGCCGACAGCCAGGCGCTGAGGCAGGCGCTTGAGCCGGGCCAGTCTCTGGTAATTGTCGGCGGTGGCCTGATC
GGTTGCGAAGTGGCGACCACTGCTATTAATGCCGGTGGCCAGTCACTGTTCTGGAGGCGGGGACGAACTGCTGTTGCGAGT
GCTAGGCCGATCAACCGGGGCTGGTGTGCAACGAGTTGGAGCGTTTGGGTGTCCGGTTGAACTGAACGCACAGGCAGCGC
ATTTTCGAGGGCGAGGGACAGTGCATGCCGTCGTTTGTGCCGATGGACGTCGGATAGCAGCTGGCACAGTTTTTGGTGAGCATC
GGTGCAAGCAGCCAGCAACTGGCAGCTGCGGCCGATTCGCATGTGAGCGCGGCTGGTAGTTGACGCTACGGGTGCAAG
CTCATGTCTCAGTATTTCGCGGCAAGTGCAGTACGCTAGCCCTGGCCCTGAGGTCCGGTGAACCTGCGCTCGCTGGAGACCTACC
TGAACAGCCACATGCAGGCTGAAACTGCCGCGCGGCCATGTTAGGCAAGTCTATCCCGGCTCTTACAGTGCCAACTCTTGG
ACGGAGATTGCAGGCATCGGATACAGATGGTTGGCGACATCGAAGGCCCGGAGAAGTTGTCTTGGCGGGTAACGTCGAGAA
TGGTCAGCCGCTGGTGCAGTTTCAAGGTTCTTGTATGTCGCGTTGAAGCCGCAACCGCTATCAATGCCCGGAAGATTTTCCCG
TTGCAACCCGATTTGGTGGCTGACCACATTCCTGTATCGGCCACAAAATTCAGGACGCTAGCTCTAACTTGGGGATTTTATG
AAAGCTAAAGCTGAGCGATGCGAGTGA
```

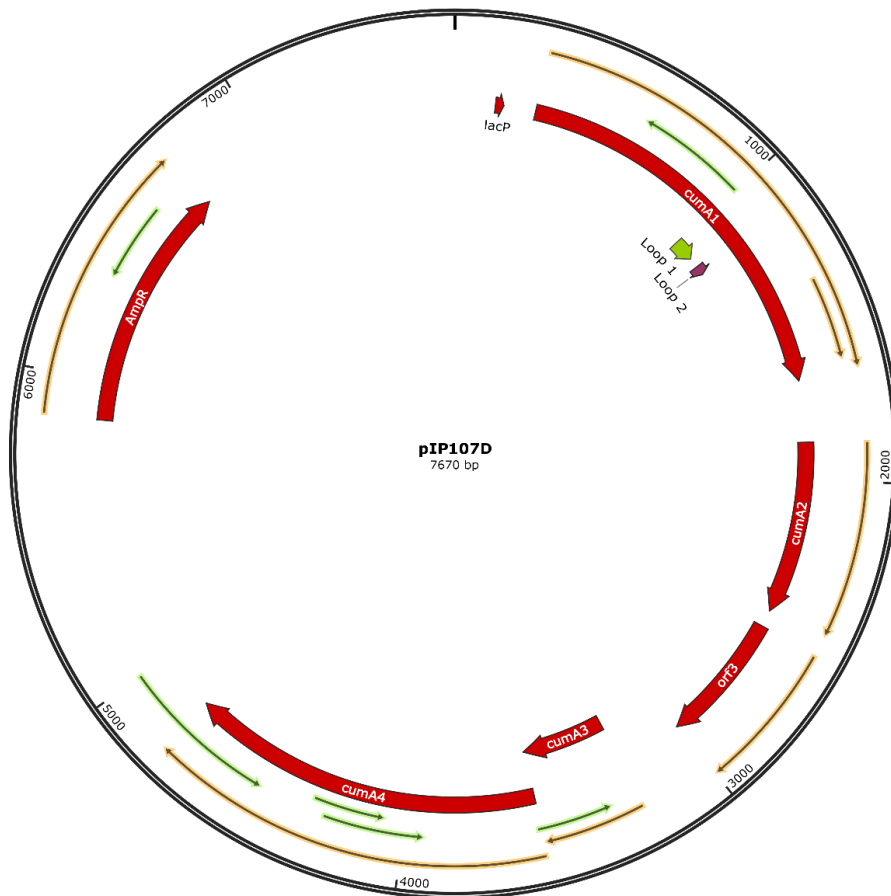


Fig. 33: Plasmid map of pIP107D.¹

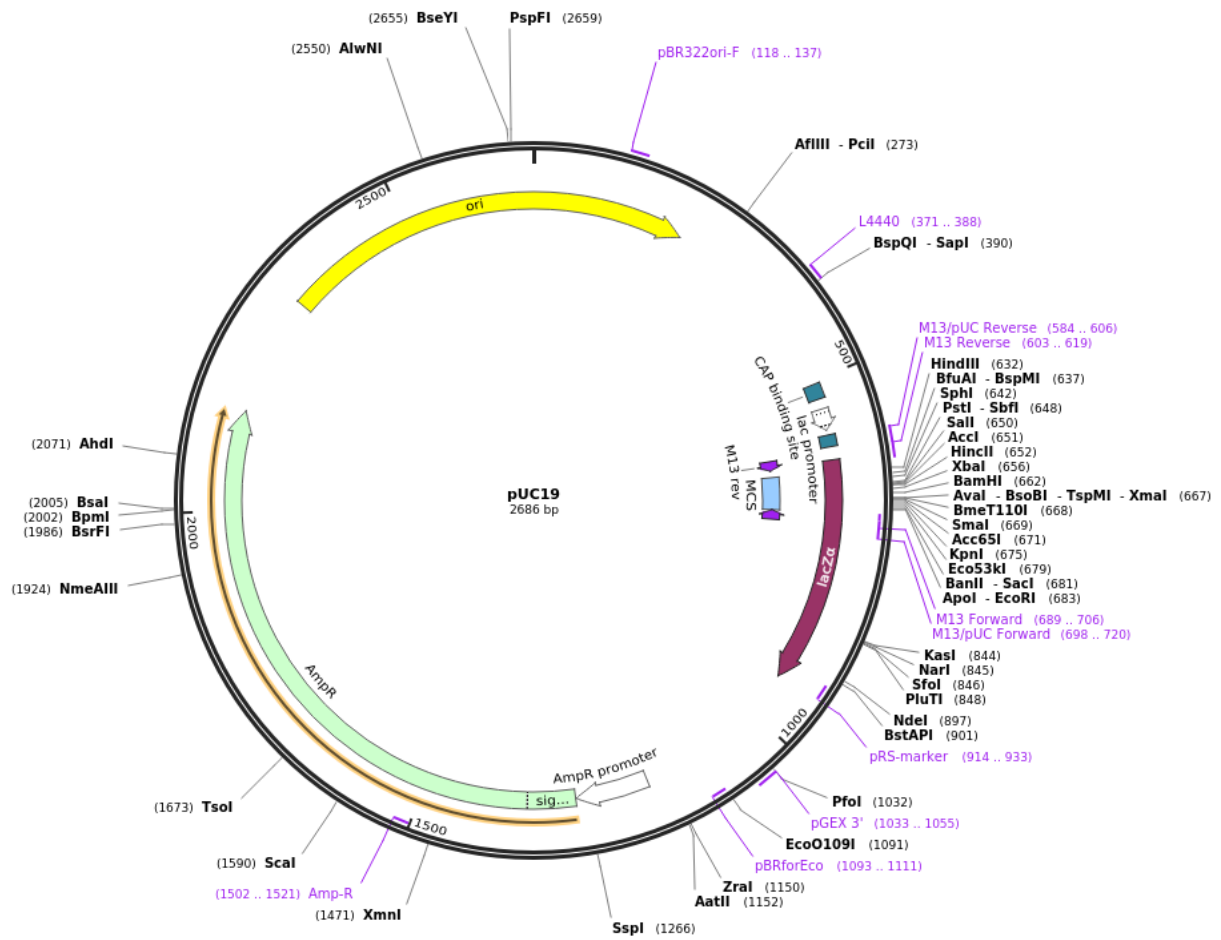


Fig. 34: Plasmid map of pUC19. (Source: <https://www.addgene.org/50005>, July 2020)

Supplementary References

1. Gally, C., Nestl, B. M. & Hauer, B. Engineering Rieske Non-Heme Iron Oxygenases for the Asymmetric Dihydroxylation of Alkenes. *Angew. Chemie - Int. Ed.* **54**, 12952–12956 (2015).
2. Halder, J. M., Nestl, B. M. & Hauer, B. Semirational Engineering of the Naphthalene Dioxygenase from *Pseudomonas* sp. NCIB 9816-4 towards Selective Asymmetric Dihydroxylation. *ChemCatChem* **10**, 178–182 (2018).
3. Vila, M. A. *et al.* Site-Directed Mutagenesis Studies on the Toluene Dioxygenase Enzymatic System: Role of Phenylalanine 366, Threonine 365 and Isoleucine 324 in the Chemo-, Regio-, and Stereoselectivity. *Adv. Synth. Catal.* **359**, 2149–2157 (2017).
4. Groeneveld, M., van Beek, H. L., Duetz, W. A. & Fraaije, M. W. Identification of a novel oxygenase capable of regiospecific hydroxylation of D-limonene into (+)-trans-carveol. *Tetrahedron* **72**, 7263–7267 (2016).
5. Boyd, D. R. *et al.* Regioselectivity and stereoselectivity of dioxygenase catalysed cis-dihydroxylation of mono- and tri-cyclic azaarene substrates. *Org. Biomol. Chem.* **6**, 3957–3966 (2008).
6. Alan, B. & Bucher, W. Menthatrienes and the Oxidation of limonene. *Helv. Chim. Acta* **53**, 770–775 (1970).
7. Scanlon, J. T. & Willis, D. E. Calculation of flame ionization detector relative response factors using the effective carbon number concept. *J. Chromatogr. Sci.* **23**, 333–340 (1985).
8. Szulejko, J. E. & Kim, K. H. Re-evaluation of effective carbon number (ECN) approach to predict response factors of ‘compounds lacking authentic standards or surrogates’ (CLASS) by thermal desorption analysis with GC-MS. *Analytica Chimica Acta* vol. 851 14–22 (2014).
9. Bermejo, F. A., Rico-Ferreira, R., Bamidele-Sanni, S. & García-Granda, S. Total synthesis of (+)-ampullicin and (+)-isoampullicin: Two fungal metabolites with growth regulatory activity isolated from *Ampulliferina* sp. 27. *J. Org. Chem.* **66**, 8287–8292 (2001).

10. Dhulut, S. *et al.* Cyclic allyl carbamates in stereoselective syn SE' processes: Synthetic approach to sarcodictyins and eleutherobin. *European J. Org. Chem.* 5235–5243 (2007) doi:10.1002/ejoc.200700490.
11. Dong, X. *et al.* Crystal Structure of the Terminal Oxygenase Component of Cumene Dioxygenase from *Pseudomonas fluorescens* IP01. *J. Bacteriol.* **187**, 2483–2490 (2005).